# SANDIA REPORT

SAND2017-6262
Unlimited Release
Printed June 2017

# Multi-compartment Aerosol Transport Model

Joshua Hubbard, Joshua Santarpia, Christopher Brotherton, Michael Omana, Danielle Rivera, and Gabriel Lucero

Prepared by
Sandia National Laboratories
Albuquerque, New Mexico 87185

Sandia National Laboratories is a multimission laboratory managed and operated by National Technology and Engineering Solutions of Sandia LLC, a wholly owned subsidiary of Honeywell International Inc. for the U.S. Department of Energy's National Nuclear Security Administration under contract DE-NA0003525.



Sandia National Laboratories

Issued by Sandia National Laboratories, operated for the United States Department of Energy by Sandia Corporation.



Available to DOE and DOE contractors from
U.S. Department of Energy
Office of Scientific and Technical Information
P.O. Box 62
Oak Ridge, TN 37831

Telephone: (865) 576-8401
Facsimile: (865) 576-5728
E-Mail: reports@osti.gov
Online ordering: http://www.osti.gov/scitech

Available to the public from
U.S. Department of Commerce
National Technical Information Service
5301 Shawnee Rd
Alexandria, VA 22312

Telephone: (800) 553-6847
Facsimile: (703) 605-6900
E-Mail: orders@ntis.gov
Online order: http://www.ntis.gov/search

SAND2017-6262
Unlimited Release
Printed June 2017

# Multi-compartment Aerosol Transport Model

Joshua Hubbard, Joshua Santarpia, Christopher Brotherton, Michael Omana, Danielle Rivera, and Gabriel Lucero

Sandia National Laboratories
P.O. Box 5800 MS 0968
Albuquerque, New Mexico 87185-MS0968

**Abstract**

A simple aerosol transport model was developed for a multi-compartmented cleanroom. Each compartment was treated as a well-mixed volume with ventilating supply and return air. Gravitational settling, intercompartment transport, and leakage of exterior air into the system were included in the model. A set of first order, coupled, ordinary differential equations was derived from the conservation equations of aerosol mass and air mass. The system of ODEs was then solved in MATLAB using pre-existing numerical methods. The model was verified against cases of (1) constant inlet-duct concentration, and (2) exponentially decaying inlet-duct concentration. Numerical methods resulted in normalized error of less than $10^{-9}$ when model solutions were compared to analytical solutions. The model was validated against experimental measurements from a single field test and showed good agreement in the shape and magnitude of the aerosol concentration profile with time.

# CONTENTS

# FIGURES

# TABLES

# 1 INTRODUCTION

A simple aerosol transport model was developed, verified, and validated, for aerosol transport in a multi-compartmented cleanroom facility where aerosol can be introduced through the main ventilating duct. The basis for this work has been the development of other aerosol transport models using the well-mixed approximation (Trost and Hubbard 2012, and Hubbard and Knowlton 2015).

A schematic representation of the current model geometry is shown in Figure 1. Aerosol concentrations were calculated in time for each of the five separate compartments. Inlet-duct concentration profiles were calculated with a simple convection algorithm accounting for gravitational aerosol transport losses in the ductwork.

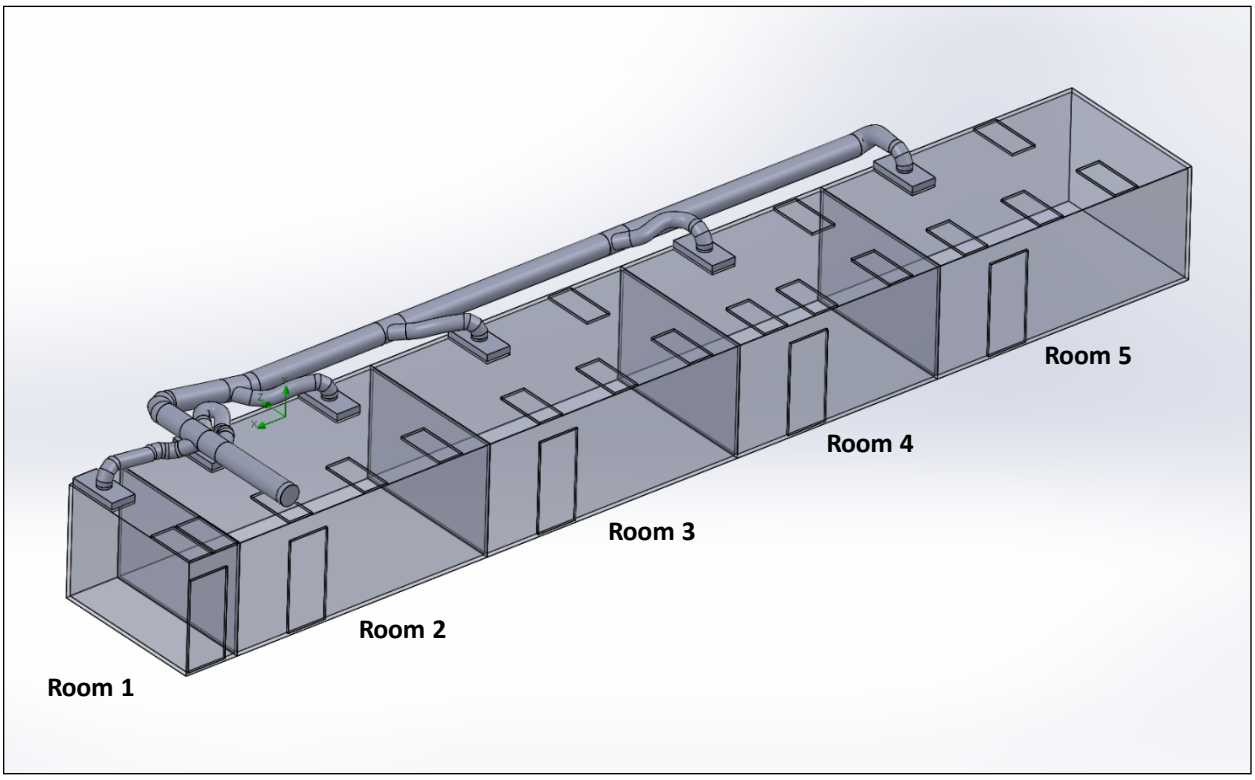


**Figure 1. Solid model representation of multi-compartmented cleanroom**

The model can be described by the following set of features.

- Each compartment was represented as a well-mixed zone (no spatial gradients in aerosol concentration within each compartment)
- Adjacent compartments were coupled by aerosol transport through cracks. Air flows through cracks were calculated with approximations for leakage areas pressure differentials between compartments.
- Gravitational settling was included as an aerosol sink term in each of the compartments.

- Aerosols could be introduced in the main ductwork of the system. Algorithms were developed to calculate time delays, and aerosol losses, as aerosols traveled through the ductwork to each of the compartments.
- Each compartment had a single supply and return ventilating duct. Duct flows were specified by measurements or could be approximated as the total air exchange rate in each compartment (e.g., ten air changes per hour).
- The entire system was assumed to be under negative pressure, and makeup air entered the system through cracks in exterior walls. Makeup air balanced supply and return air flow rates and had an aerosol concentration equal to the background aerosol concentration (non-zero). This was an important feature as the background concentration is rarely zero and asymptotic behavior ($t \to \infty$) looked peculiar unless the background concentration is incorporated into the model.
- Initial aerosol concentrations in each of the compartments could be specified.
- Compartment 5 had a recirculation loop with a filter element to remove particulate. The other compartments did not have recirculation loops.
- The set of first order, coupled, ordinary differential equations was solved in MATLAB using pre-existing numerical methods.
- The model was verified against cases of (1) constant inlet-duct concentration, and (2) exponentially decaying inlet-duct concentration. Numerical methods resulted in normalized error of less than $10^{-9}$.
- The model was validated against experimental measurements from a single field test and showed good agreement in the shape and magnitude of the aerosol concentration profile with time.

# 2 MODEL DEVELOPMENT

## 2.1 Schematic

A schematic of the compartments, and air flows, is shown in Figure 2 where nomenclature is given below the figure.

### *2.1.1 Compartments*

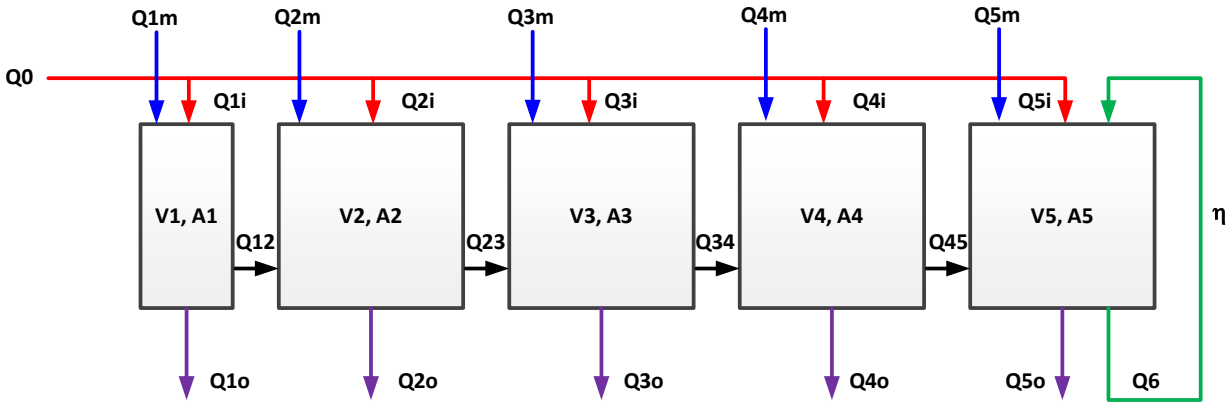


**Figure 2. Schematic of multicompartment aerosol transport model with five separate volumes.**

| | |
|---|---|
| Q0 | total air flow rate entering the main HVAC plenum |
| Q1i | specific air flow rate entering compartment 1 off the HVAC plenum (supply) |
| Q1o | specific air flow rate leaving compartment 1 (return) |
| V1 | volume of compartment 1 |
| A1 | floor area of compartment 1 |
| Q12 | leakage flow rate from compartment 1 to compartment 2 driven by pressure differential |
| Q1m | makeup air flow rate in to compartment 1 from exterior of system (assumes that system is always under negative pressure and some makeup air is always introduced into the system) |
| Q6 | recirculation air flow rate in compartment 5 |
| η | efficiency of filter unit in recirculation duct of compartment 5 |

### 2.1.2 Ductwork

A simple algorithm was used to calculated inlet-duct (supply) aerosol concentration profiles. The algorithm utilized specified air flow rates, duct diameters, duct lengths, and gravitational settling to calculate time delays and transport losses as aerosols were transported to each of the compartments. This was possible since each compartment was fed through a series of ducts with known characteristics. More rigorous methods could be applied to duct flows but were not included in the present model.

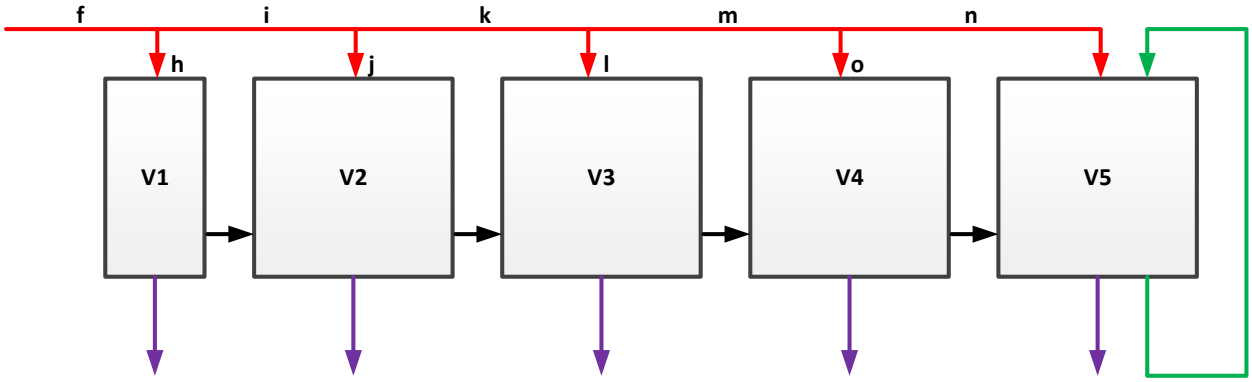


**Figure 3. Ductwork segment nomenclature for inlet concentration profile algorithm (f,h,I,j,k,l,m,n,o)**

An example calculation is provided for the duct node downstream of segment *f*. If the aerosol release is $0 < t < 180$ seconds, the characteristic transport time $\tau$ of segment *f* determines the time over which the concentration at that node is non-zero.

$$\tau = \frac{U}{L} = \frac{Q}{\frac{\pi}{4} D^2 L} \qquad \text{* MERGEFORMAT (1)}$$

In * MERGEFORMAT (1), $U$ is bulk air velocity, $L$ is duct length, $Q$ is air flow rate, and $D$ is duct diameter. Transmission efficiencies, $\eta_{transport}$, in each segment were calculated according to the following:

$$\eta_{transport} = \exp\left(-\frac{DLv_t}{Q}\right). \qquad \text{* MERGEFORMAT (2)}$$

Equation * MERGEFORMAT (2) is valid for turbulent flow in a horizontal tube as given in Brockmann (2011). A representative characteristic transport time for the system is on the order of a few seconds when standard air exchange rates are used (~ 10 air changes per hour). For 10 μm particles with a density of 4230 kg/m$^3$, transport efficiencies range from 78-99%. Transport efficiencies are greater than 99% for 2 μm particles with the same density. Time delays and transport efficiencies may be non-negligible at lower air exchange rates (~ 1 air change per hour).

## 2.2 Conservation Laws

The basis for this aerosol transport model is the conservation of mass. Sets of equations were derived from the conservation of particle mass, and the conservation of air mass. Each volume was assumed to be well-mixed.

### *2.2.1 Particle Mass*

The change in aerosol mass in a compartment, per unit time, is equal to the mass flow balance. The volume of each compartment is not a function of time, thus, the change in mass per unit time becomes the change in aerosol concentration per unit time. Gravitational losses show up in these equations as a sink term along with the return air flow rate. Intercompartment leakage terms serve as a sink for one compartment and a source for the adjacent compartment. Makeup air flow rates bring in an aerosol with background concentration, $C_{bg}$ . Only * MERGEFORMAT (7) contains a reference to the recirculation flow rate and filter efficiency.

$$\frac{dm_1}{dt} = V_1 \frac{dC_1}{dt} = Q_{1i}C_i + Q_{1m}C_{bg} - C_1(Q_{12} + v_t A_1 + Q_{1o}) \quad \text{* MERGEFORMAT (3)}$$

$$\frac{dm_2}{dt} = V_2 \frac{dC_2}{dt} = Q_{2i}C_i + Q_{2m}C_{bg} + Q_{12}C_1 - C_2(Q_{23} + v_t A_2 + Q_{2o}) \quad \text{* MERGEFORMAT (4)}$$

$$\frac{dm_3}{dt} = V_3 \frac{dC_3}{dt} = Q_{3i}C_i + Q_{3m}C_{bg} + Q_{23}C_2 - C_3(Q_{34} + v_t A_3 + Q_{3o}) \quad \text{* MERGEFORMAT (5)}$$

$$\frac{dm_4}{dt} = V_4 \frac{dC_4}{dt} = Q_{4i}C_i + Q_{4m}C_{bg} + Q_{34}C_3 - C_4(Q_{45} + v_t A_4 + Q_{4o}) \quad \text{* MERGEFORMAT (6)}$$

$$\frac{dm_5}{dt} = V_5 \frac{dC_5}{dt} = Q_{5i}C_i + Q_{5m}C_{bg} + Q_{45}C_4 - C_5(v_t A_5 + Q_{5o} + \eta Q_6) \quad \text{* MERGEFORMAT (7)}$$

### *2.2.2 Air Mass*

The model was setup such that supply and return air flow rates are specified. In field testing, return air flow rates were approximately twice as high as supply air flow rates. The excess air flow (not supplied) came from the exterior of the compartments through crack leakage. This occurred since the compartments were held at negative pressure. Makeup air flow rates were therefore calculated.

$$Q_{1m} = -Q_{1i} + Q_{12} + Q_{1o} \quad \text{* MERGEFORMAT (8)}$$

$$Q_{2m} = -Q_{2i} - Q_{12} + Q_{23} + Q_{2o} \quad \text{* MERGEFORMAT (9)}$$

$$Q_{3m} = -Q_{3i} - Q_{23} + Q_{34} + Q_{3o} \quad \text{* MERGEFORMAT (10)}$$

$$Q_{4m} = -Q_{4i} - Q_{34} + Q_{45} + Q_{4o} \quad \text{* MERGEFORMAT (11)}$$

$$Q_{4m} = -Q_{5i} - Q_{45} + Q_{5o} \quad \text{* MERGEFORMAT (12)}$$

## 2.3 Intercompartment Leakage Air Flow Rate

Air transfer from one compartment to the next is driven by pressure differentials between the compartments. The formulation of Walker et al. (1998) was used to calculate air flow rates from pressure differences:

$$Q_{12} = \frac{-A + \sqrt{A^2 + 4B\Delta P_{12}}}{2B} \qquad \text{* MERGEFORMAT (13)}$$

where

$$A = \frac{12\mu z_{crack}}{L_{crack} d_{crack}^{\ 3}} \qquad \text{* MERGEFORMAT (14)}$$

and

$$B = \frac{\rho Y}{2 d_{crack}^{\ 2} L_{crack}^{\ 2}}. \qquad \text{* MERGEFORMAT (15)}$$

In * MERGEFORMAT (13), * MERGEFORMAT (14), and * MERGEFORMAT (15), $\mu$ is the dynamic air viscosity, $z_{crack}$ is the distance in the flow direction (taken as 0.038 meters or 1.5 inches), $L_{crack}$ is the width of the crack (taken as 6.1 meters or 20 feet), $d_{crack}$ is the gap thickness (taken as 0.001 meters or 3/8 inches), $\rho$ is air density, and $Y$ is a constant of 1.5 for a straight crack. These dimensions were approximated for a single standard door in between compartments. Pressure differentials are specified in Pascals. For a pressure difference of 1 Pa, the flow would be 0.06 $m^3/s$ or approximately 3.8 air changes per hour in compartment 2.

## 2.4 Numerical Methods

Inlet-duct (supply) concentration profiles are first calculated for an arbitrary time vector. The minimum and maximum times, and time step are specified by the user. The ODE solver returns concentration values at the specified time intervals. Initial compartment concentrations, the inlet-duct concentration profiles, and other parameters are then sent to the ODE45 function in MATLAB. Equations * MERGEFORMAT (3) through * MERGEFORMAT (7) were written in a MATLAB format compatible with the ODE solver. The ODE solver relative and absolute tolerances were set to $10^{-9}$ and $10^{-12}$, respectively. MATLAB defines the relative tolerance as "*a measure of the error relative to the size of each solution component. Roughly, it controls the number of correct digits in all solution components, except those smaller than the absolute tolerance threshold*". MATLAB defines the absolute tolerance as "*a threshold below which the value of the $i^{th}$ solution component is unimportant. The absolute error tolerances determine the accuracy when the solution approaches zero*". In practice the tolerances were adjusted to give acceptable values in normalized error when model results were compared to analytical solutions (model verification).

# 3 MODEL VERIFICATION

Model verification was first performed to determine if algorithms and numerical methods had been implemented correctly. The code was verified against analytical solutions to ensure the MATLAB routines were functioning as expected. Model verification does not gage the model's ability to simulate proper physics (which is referred to as model validation).

## 3.1 Constant Duct-Inlet Condition

The simplest model verification case is where inlet-duct concentrations are independent of time. Inlet-duct concentrations were specified as $100C_{bg}$ where $C_{bg}$ = 10 particles per cm$^3$ or $10^7$ particles per m$^3$. The value of background concentration was taken from experimental data in compartment 3. Model verification can only be performed when the compartments are decoupled, i.e., there were no intercompartment transport terms. Coupled ODEs require numerical methods.

### *3.1.1 Analytical Solution*

The solutions to each of the five, independent, first order ODEs were broken into homogenous ($C_h$) and particular ($C_p$) solutions:

$$C = C_h + C_p . \qquad \text{* MERGEFORMAT (16)}$$

For the case of constant inlet-duct concentration, the particular solution was assumed to be of the form

$$C_p = \text{constant} . \qquad \text{* MERGEFORMAT (17)}$$

The analytical solution for compartments 1 and 5 are given by

$$C_1(t) = \left[\left(C_{1,init} - \frac{Q_{1i}C_i + Q_{1c}C_{bg}}{Q_{1o} + v_t A_1}\right)\exp\left(-\left(\frac{Q_{1o} + v_t A_1}{V_1}\right)t\right)\right] + \left(\frac{Q_{1i}C_i + Q_{1c}C_{bg}}{Q_{1o} + v_t A_1}\right), \text{* MERGEFORMAT (18}$$

and

$$C_5(t) = \left[\left(C_{5,init} - \frac{Q_{5i}C_i + Q_{5c}C_{bg}}{Q_{5o} + v_t A_5 + \eta Q_6}\right)\exp\left(-\left(\frac{Q_{5o} + v_t A_5 + \eta Q_6}{V_5}\right)t\right)\right] + \left(\frac{Q_{5i}C_i + Q_{5m}C_{bg}}{Q_{5o} + v_t A_5 + \eta Q_6}\right), \text{* MERGEFORMA}$$

respectively. Solutions for compartments 2,3, and 4 look like * MERGEFORMAT (18). Two verification cases are provided below. The normalized error ($\hat{e}$) of the numerical solutions were calculated according to

$$\hat{e} = \frac{\left| C_{numerical} - C_{analytical} \right|}{C_{analytical}} . \qquad \text{* MERGEFORMAT (20)}$$

This formulation provides the error relative to the magnitude of the true solution (analytical solution). The relative and absolute tolerances of the ODE45 MATLAB routine were specified such that the normalized errors were less than $10^{-9}$.

### *3.1.2 Test Case: Without Recirculation Flow in Compartment 5*

#### 3.1.2.1 Inputs

```
dp_array=10.0e-6;
    %SystemGeometry
(A=Area,Vo=Volume)

A1=((3+10.625/12)*0.3048)*(12*0.304
8); %m^2
    Vo1=A1*(8*0.3048); %m^3

A2=((20+1.125/12)*0.3048)*(12*0.304
8); %m^2
    Vo2=A2*(8*0.3048); %m^3

A3=((20+1.125/12)*0.3048)*(12*0.304
8); %m^2
    Vo3=A3*(8*0.3048); %m^3

A4=((16+0.5/12)*0.3048)*(12*0.3048)
; %m^2
    Vo4=A4*(8*0.3048); %m^3

A5=((20+1.125/12)*0.3048)*(12*0.304
8); %m^2
    Vo5=A5*(8*0.3048); %m^2
    %Atmospheric pressure (Pa) and
temperature (K)
    P=101325;
    T=293.15;
    %Particle size distribution
    %Particle diameter (m)
    dp = dp_array(i);
    %Particle density (kg/m^3)
    rhop=4230.0;
    %Duration of particle release s
    t_release=3*60;
    %Mass of material released (kg)
    mass_0=0.005;
    %Inlet-duct (supply) air flow
rates (m^3/s)
    Q1i=5*Vo1/3600;
    Q2i=0.1557;
    Q3i=0.1463;
    Q4i=0.1312;
    Q5i=0.0958;
    %Exhaust-duct (return) air flow
rates (m^3/s)
    Q1o=10*Vo1/3600;
    Q2o=0.2416;
    Q3o=0.2388;
    Q4o=0.2364;
    Q5o=0.2431;
    %Filtration efficiency on
recirculation duct (unitless)
    eta=1.0;
    %Recirculation duct air flow
rate (m^3/s)
    Q6o=0.0;
    %Pressure differential between
adjacent rooms (Pa)
    dP12=0.0;
    dP23=0.0;
    dP34=0.0;
    dP45=0.0;
    %Calculation crack leakage flow
rates (m^3/s)
    Q12=crack_leakage_flow(dP12);
    Q23=crack_leakage_flow(dP23);
    Q34=crack_leakage_flow(dP34);
    Q45=crack_leakage_flow(dP45);
    %Makeup air flow rates coming
from exterior of cleanroom (m^3/s)
    Q1m = Q12+Q1o-Q1i;
    Q2m = -Q2i-Q12+Q23+Q2o;
    Q3m = -Q3i-Q23+Q34+Q3o;
    Q4m = -Q4i-Q34+Q45+Q4o;
    Q5m = -Q5i-Q45+Q5o;
    %Background aerosol
concentration outside
cleanroom(#/m^3)
    Cbg = 10*1e6;
    %Initial aerosol concentration
(#/m^3)
    C1init=Cbg;
    C2init=Cbg;
    C3init=Cbg;
    C4init=Cbg;
    C5init=Cbg;
```

### 3.1.2.2 Results

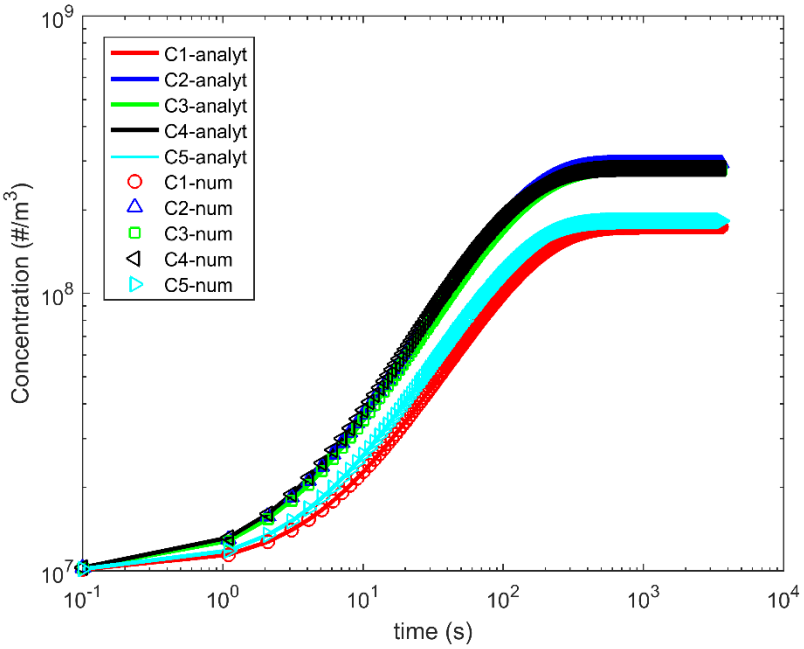


**Figure 4. Aerosol concentration vs. time for (1) constant inlet concentration and (2) without recirculation in compartment 5**

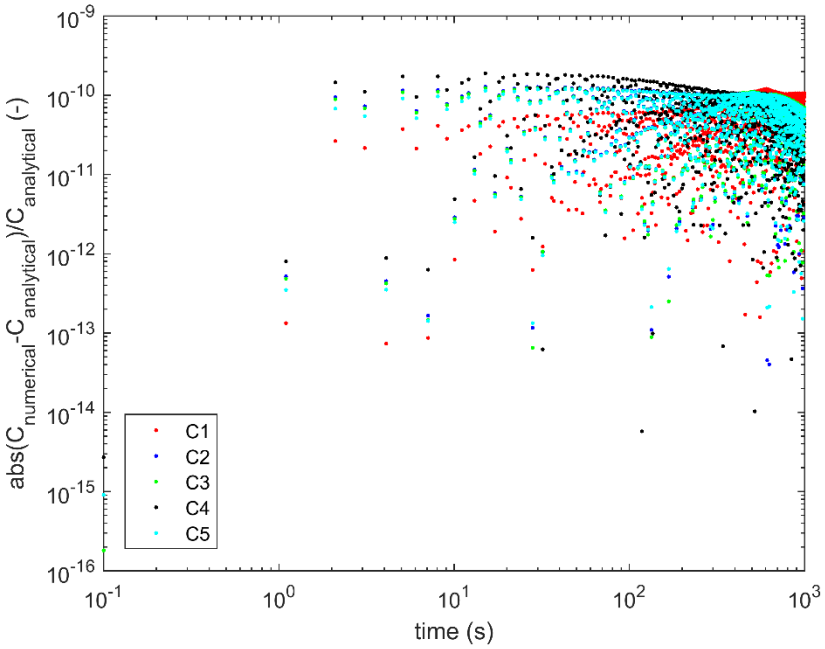


**Figure 5. Absolute difference between numerical and analytical solutions normalized by the analytical solution for (1) constant inlet concentration and (2) without recirculation in compartment 5**

### *3.1.3 Test Case: With Recirculation Flow in Compartment 5*

#### 3.1.3.1 Inputs

```
    dp_array=2.5e-6;
    %System                 Geometry
(A=Area,Vo=Volume)

A1=((3+10.625/12)*0.3048)*(12*0.304
8); %m^2
    Vo1=A1*(8*0.3048); %m^3

A2=((20+1.125/12)*0.3048)*(12*0.304
8); %m^2
    Vo2=A2*(8*0.3048); %m^3

A3=((20+1.125/12)*0.3048)*(12*0.304
8); %m^2
    Vo3=A3*(8*0.3048); %m^3

A4=((16+0.5/12)*0.3048)*(12*0.3048)
; %m^2
    Vo4=A4*(8*0.3048); %m^3

A5=((20+1.125/12)*0.3048)*(12*0.304
8); %m^2
    Vo5=A5*(8*0.3048); %m^2
    %Atmospheric pressure (Pa) and
temperature (K)
    P=101325;
    T=293.15;
    %Particle size distribution
    %Particle diameter (m)
    dp = dp_array(i);
    %Particle density (kg/m^3)
    rhop=4230.0;
    %Duration of particle release
(s)
    t_release=3*60;
    %Mass of material released (kg)
    mass_0=0.005;
    %Inlet-duct (supply) air flow
rates (m^3/s)
    Q1i=5*Vo1/3600;
    Q2i=0.1557;
    Q3i=0.1463;
    Q4i=0.1312;
    Q5i=0.0958;
    %Exhaust-duct (return) air flow
rates (m^3/s)
    Q1o=10*Vo1/3600;
    Q2o=0.2416;
    Q3o=0.2388;
    Q4o=0.2364;
    Q5o=0.2431;
      %Filtration efficiency on
      recirculation duct (unitless)
    eta=1.0;
    %Recirculation duct air flow
rate (m^3/s)
    Q6o=100*Vo5/3600;
      %Pressure differential
      between adjacent rooms (Pa)
    dP12=0.0;
    dP23=0.0;
    dP34=0.0;
    dP45=0.0;
    %Calculation crack leakage flow
rates (m^3/s)
    Q12=crack_leakage_flow(dP12);
    Q23=crack_leakage_flow(dP23);
    Q34=crack_leakage_flow(dP34);
    Q45=crack_leakage_flow(dP45);
      %Makeup air flow rates coming
      from exterior of cleanroom
      (m^3/s)
    Q1m = Q12+Q1o-Q1i;
    Q2m = -Q2i-Q12+Q23+Q2o;
    Q3m = -Q3i-Q23+Q34+Q3o;
    Q4m = -Q4i-Q34+Q45+Q4o;
    Q5m = -Q5i-Q45+Q5o;
      %Background aerosol
      concentration outside
      cleanroom(#/m^3)
    Cbg = 10*1e6;
    %Initial aerosol concentration
(#/m^3)
    C1init=Cbg;
    C2init=Cbg;
    C3init=Cbg;
    C4init=Cbg;
    C5init=Cbg;
```

### 3.1.3.2 Results

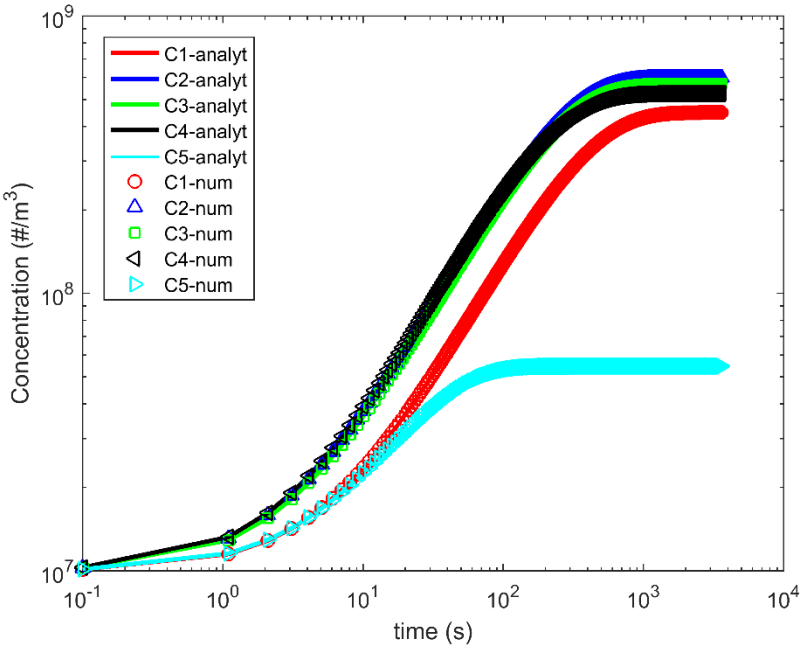


**Figure 6. Aerosol concentration vs. time for (1) constant inlet concentration and (2) with recirculation in compartment 5**

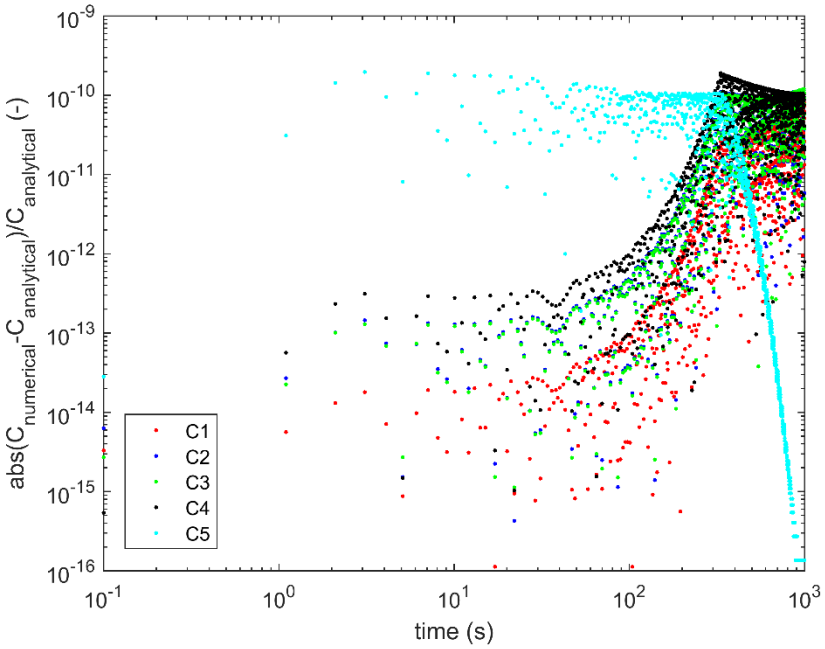


**Figure 7. Absolute difference between numerical and analytical solutions normalized by the analytical solution for (1) constant inlet concentration and (2) with recirculation in compartment 5**

## 3.2 Exponentially Decaying Duct-Inlet Condition

A more complex verification case is a time-dependent inlet-duct aerosol concentration profile. For simple functions, like exponential decay, the ODEs have analytical solutions. Numerical methods are required for arbitrary or complex inlet-duct concentration profiles, hence the need for this numerical model. The time vector used to specify the inlet-duct concentration profiles should be sufficiently high in resolution to represent the inlet-duct concentration profile when it is rapidly changing. This is due to the fact that inlet-duct concentration profiles are interpolated at ODE solver time steps.

### *3.2.1 Analytical Solution*

We assume the inlet concentration profile is exponentially decaying to the background concentration where there are two arbitrary constants $C_1$ and $C_2$

$$C_i(t) = C_1 \exp\left(-C_2 t\right) + C_{bg} \ . \qquad \text{* MERGEFORMAT (21)}$$

Again, we break the ODE solution into homogeneous and particular solutions. The particular solution for the inlet-duct concentration profile of * MERGEFORMAT (21) is assumed to be of the following form

$$C_p = \alpha \exp\left(-C_2 t\right) + \varepsilon \ . \qquad \text{* MERGEFORMAT (22)}$$

The solution to the ODE for compartment 1 is given by

$$C_1(t) = \gamma \exp\left( -\frac{Q_{1o} + v_t A_1}{V_1} t \right) + \alpha \exp\left(-C_2 t\right) + \varepsilon \ \text{* MERGEFORMAT (23)}$$

where

$$\alpha = \frac{\left( \frac{Q_{1i} C_1}{V_1} \right)}{\left( \frac{Q_{1o} + v_t A_1}{V_1} \right) - C_2}, \qquad \text{* MERGEFORMAT (24)}$$

$$\varepsilon = \frac{\left( \frac{Q_{1i} + Q_{1m}}{V_1} \right) C_{bg}}{\left( \frac{Q_{1o} + v_t A_1}{V_1} \right)} \text{, and} \qquad \text{* MERGEFORMAT (25)}$$

$$\gamma = C_{bg} - \alpha - \varepsilon \ . \qquad \text{* MERGEFORMAT (26)}$$

The solution for compartment 5 can be written by making the appropriate substitutions for volumes, areas, flow rates, and $Q_{1o} + v_t A_1 \rightarrow Q_{5o} + v_t A_5 + \eta Q_6$. Two test cases are given below where analytical and numerical solutions, and normalized error, are plotted. Model results are in excellent agreement with the analytical solution.

### *3.2.2 Test Case: Without Recirculation Flow in Compartment 5*

#### 3.2.2.1 Inputs

```
    dp_array=10.0e-6;
    %System                 Geometry
(A=Area,Vo=Volume)

A1=((3+10.625/12)*0.3048)*(12*0.304
8); %m^2
    Vo1=A1*(8*0.3048); %m^3

A2=((20+1.125/12)*0.3048)*(12*0.304
8); %m^2
    Vo2=A2*(8*0.3048); %m^3

A3=((20+1.125/12)*0.3048)*(12*0.304
8); %m^2
    Vo3=A3*(8*0.3048); %m^3

A4=((16+0.5/12)*0.3048)*(12*0.3048)
; %m^2
    Vo4=A4*(8*0.3048); %m^3

A5=((20+1.125/12)*0.3048)*(12*0.304
8); %m^2
    Vo5=A5*(8*0.3048); %m^2
    %Atmospheric pressure (Pa) and
temperature (K)
    P=101325;
    T=293.15;
    %Particle size distribution
    %Particle diameter (m)
    dp = dp_array(i);
    %Particle density (kg/m^3)
    rhop=4230.0;
    %Duration of particle release
(s)
    t_release=3*60;
    %Mass of material released (kg)
    mass_0=0.005;
    %Inlet-duct (supply) air flow
rates (m^3/s)
    Q1i=5*Vo1/3600;
    Q2i=0.1557;
    Q3i=0.1463;
    Q4i=0.1312;
    Q5i=0.0958;
    %Exhaust-duct (return) air flow
rates (m^3/s)
    Q1o=10*Vo1/3600;
    Q2o=0.2416;
    Q3o=0.2388;
    Q4o=0.2364;
    Q5o=0.2431;
      %Filtration efficiency on
      recirculation duct (unitless)
    eta=1.0;
    %Recirculation duct air flow
rate (m^3/s)
    Q6o = 0.0;
      %Pressure         differential
      between adjacent rooms (Pa)
    dP12=0.0;
    dP23=0.0;
    dP34=0.0;
    dP45=0.0;
    %Calculation crack leakage flow
rates (m^3/s)
    Q12=crack_leakage_flow(dP12);
    Q23=crack_leakage_flow(dP23);
    Q34=crack_leakage_flow(dP34);
    Q45=crack_leakage_flow(dP45);
      %Makeup air flow rates coming
      from exterior of cleanroom
      (m^3/s)
    Q1m = Q12+Q1o-Q1i;
    Q2m = -Q2i-Q12+Q23+Q2o;
    Q3m = -Q3i-Q23+Q34+Q3o;
    Q4m = -Q4i-Q34+Q45+Q4o;
    Q5m = -Q5i-Q45+Q5o;
      %Background           aerosol
      concentration        outside
      cleanroom(#/m^3)
    Cbg = 10*1e6;
    %Initial aerosol concentration
(#/m^3)
    C1init=Cbg;
    C2init=Cbg;
    C3init=Cbg;
    C4init=Cbg;
    C5init=Cbg;
```

### 3.2.2.2 Results

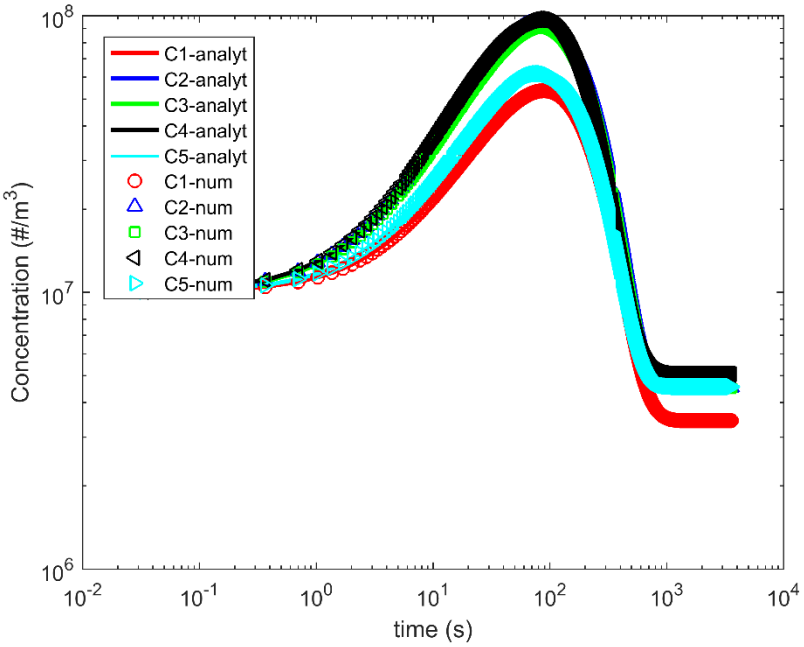


**Figure 8. Aerosol concentration vs. time for (1) exponentially decaying inlet concentration and (2) without recirculation in compartment 5**

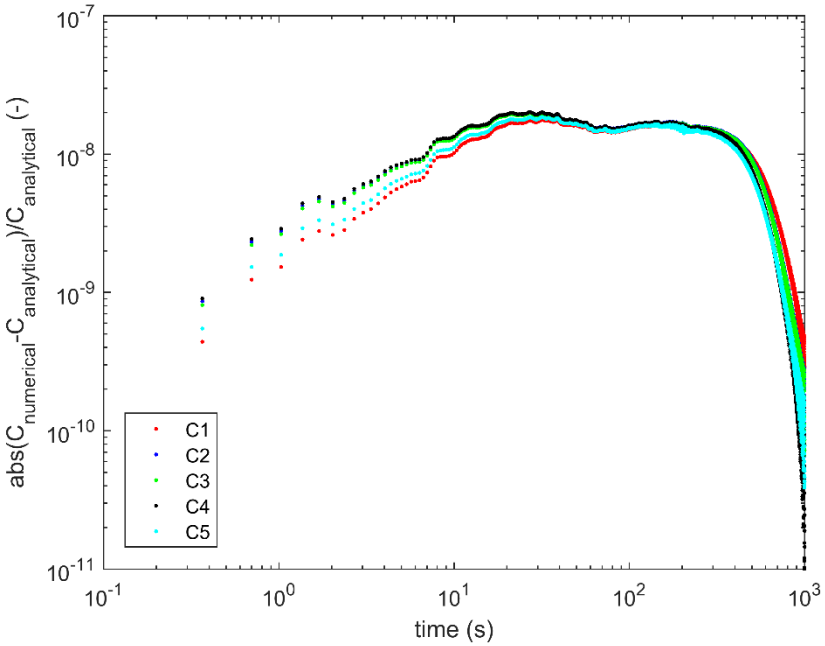


**Figure 9. Absolute difference between numerical and analytical solutions normalized by the analytical solution for (1) exponentially decaying inlet concentration and (2) without recirculation in compartment 5**

### *3.2.3 Test Case: With Recirculation Flow in Compartment 5*

#### 3.2.3.1 Inputs

```
    dp_array=1.0e-6;
    %System                 Geometry
(A=Area,Vo=Volume)

A1=((3+10.625/12)*0.3048)*(12*0.304
8); %m^2
    Vo1=A1*(8*0.3048); %m^3

A2=((20+1.125/12)*0.3048)*(12*0.304
8); %m^2
    Vo2=A2*(8*0.3048); %m^3

A3=((20+1.125/12)*0.3048)*(12*0.304
8); %m^2
    Vo3=A3*(8*0.3048); %m^3

A4=((16+0.5/12)*0.3048)*(12*0.3048)
; %m^2
    Vo4=A4*(8*0.3048); %m^3

A5=((20+1.125/12)*0.3048)*(12*0.304
8); %m^2
    Vo5=A5*(8*0.3048); %m^2
    %Atmospheric pressure (Pa) and
temperature (K)
    P=101325;
    T=293.15;
    %Particle size distribution
    %Particle diameter (m)
    dp = dp_array(i);
    %Particle density (kg/m^3)
    rhop=4230.0;
    %Duration of particle release
(s)
    t_release=3*60;
    %Mass of material released (kg)
    mass_0=0.005;
    %Inlet-duct (supply) air flow
rates (m^3/s)
    Q1i=5*Vo1/3600;
    Q2i=0.1557;
    Q3i=0.1463;
    Q4i=0.1312;
    Q5i=0.0958;
    %Exhaust-duct (return) air flow
rates (m^3/s)
    Q1o=10*Vo1/3600;
    Q2o=0.2416;
    Q3o=0.2388;
    Q4o=0.2364;
    Q5o=0.2431;
      %Filtration efficiency on
      recirculation duct (unitless)
    eta=1.0;
    %Recirculation duct air flow
rate (m^3/s)
    %Q6o = 0.0;
    Q6o=100*Vo5/3600;
      %Pressure differential
      between adjacent rooms (Pa)
    dP12=0.0;
    dP23=0.0;
    dP34=0.0;
    dP45=0.0;
    %Calculation crack leakage flow
rates (m^3/s)
    Q12=crack_leakage_flow(dP12);
    Q23=crack_leakage_flow(dP23);
    Q34=crack_leakage_flow(dP34);
    Q45=crack_leakage_flow(dP45);
      %Makeup air flow rates coming
      from exterior of cleanroom
      (m^3/s)
    Q1m = Q12+Q1o-Q1i;
    Q2m = -Q2i-Q12+Q23+Q2o;
    Q3m = -Q3i-Q23+Q34+Q3o;
    Q4m = -Q4i-Q34+Q45+Q4o;
    Q5m = -Q5i-Q45+Q5o;
      %Background aerosol
      concentration outside
      cleanroom(#/m^3)
    Cbg = 10*1e6;
    %Initial aerosol concentration
(#/m^3)
    C1init=Cbg;
    C2init=Cbg;
    C3init=Cbg;
    C4init=Cbg;
    C5init=Cbg;
```

### 3.2.3.2 Results

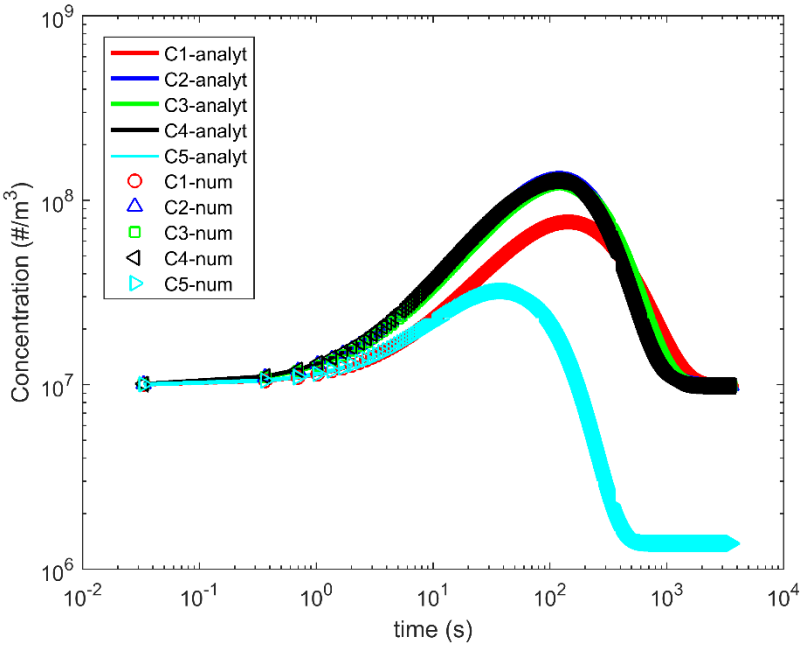


**Figure 10. Aerosol concentration vs. time for (1) exponentially decaying inlet concentration and (2) with recirculation in compartment 5**

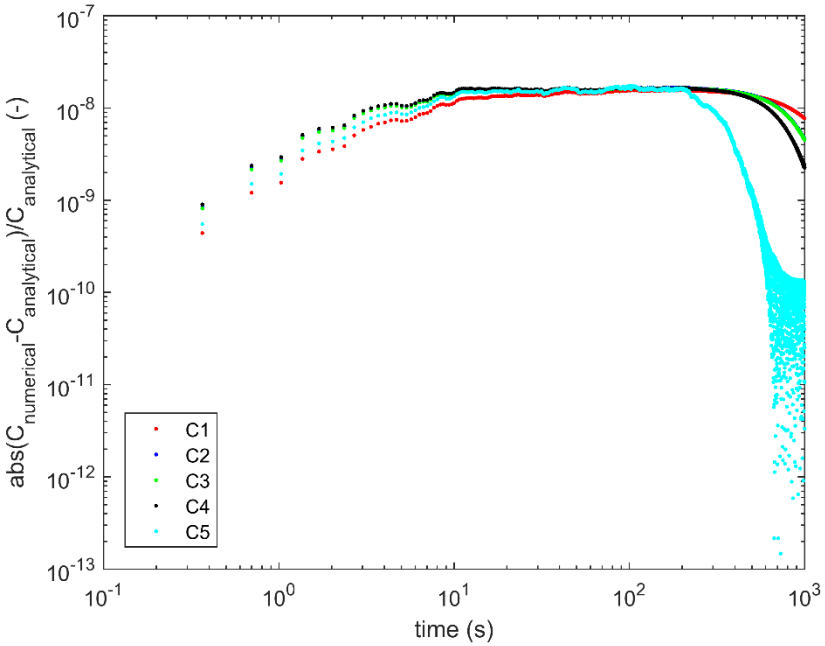


**Figure 11. Absolute difference between numerical and analytical solutions normalized by the analytical solution for (1) exponentially decaying inlet concentration and (2) with recirculation in compartment 5**

# 4 MODEL VALIDATION

The model was developed to represent an existing system with available test data. The model was therefore validated against experimental data from a single test conducted in April of 2015. Model validation gages whether the model is representative of actual physical processes.

## 4.1 Schematics

Dimensions for the multi-compartmented cleanroom facility are shown in Figure 12 and Figure 13. Compartment 1 (model nomenclature) is shown on the far left. Compartment 1 is approximately 4 feet wide. Compartments 2, 3, and 5 are approximately 20 feet wide. Compartment 4 is approximately 16 feet wide. There are multiple supply and return vent ducts but each compartment is only modeled with one since compartments are approximated as well-mixed.

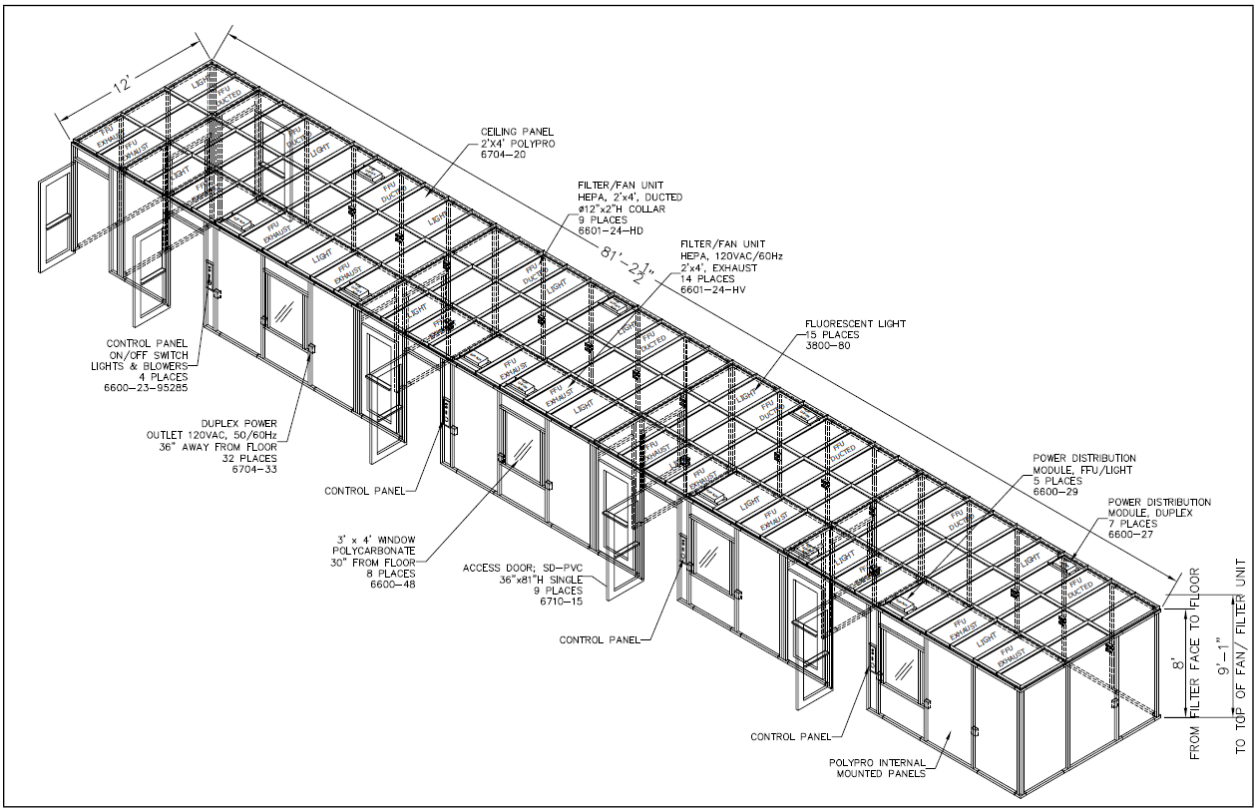


**Figure 12. Dimensions of multi-compartmented cleanroom (iso)**

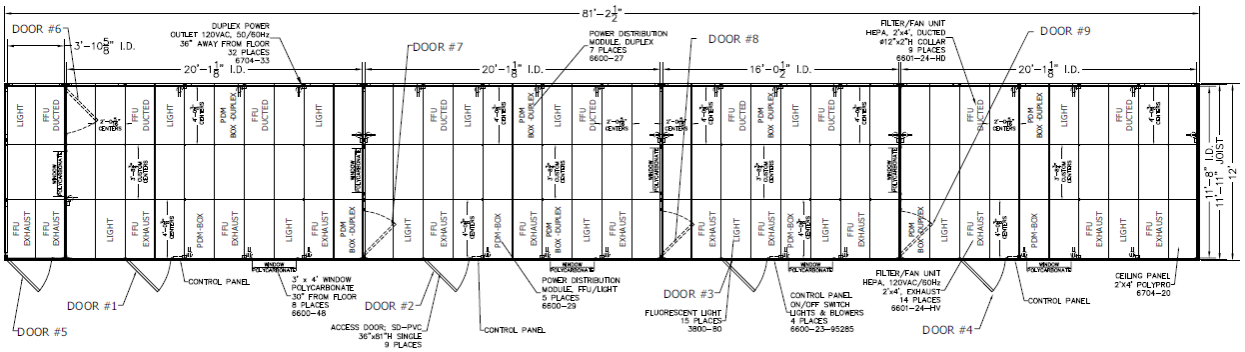


**Figure 13. Dimensions of multi-compartmented cleanroom (plan)**

In experiments, the ventilation to compartment 1 was shut off. Compartments 2 through 5 were instrumented with AeroTrak Remote Particle Counters (model 7310). The AeroTrak reports up to 4 particle sizes simultaneously from 0.3-10 µm. AeroTrak numbers are shown in Figure 14. Room 2 contains AeroTraks 201-205. Room 3 contains AeroTraks 206-210. A TSI Aerodynamic Particle Sizer (TSI 3321) was collocated with AeroTrak 208 in experiments. Compartment 3 will be the focus of model validation since APS measurements were made in that compartment. AeroTrak 101 was located in the ductwork near the point of aerosol release and was used to define time-zero in the data files.

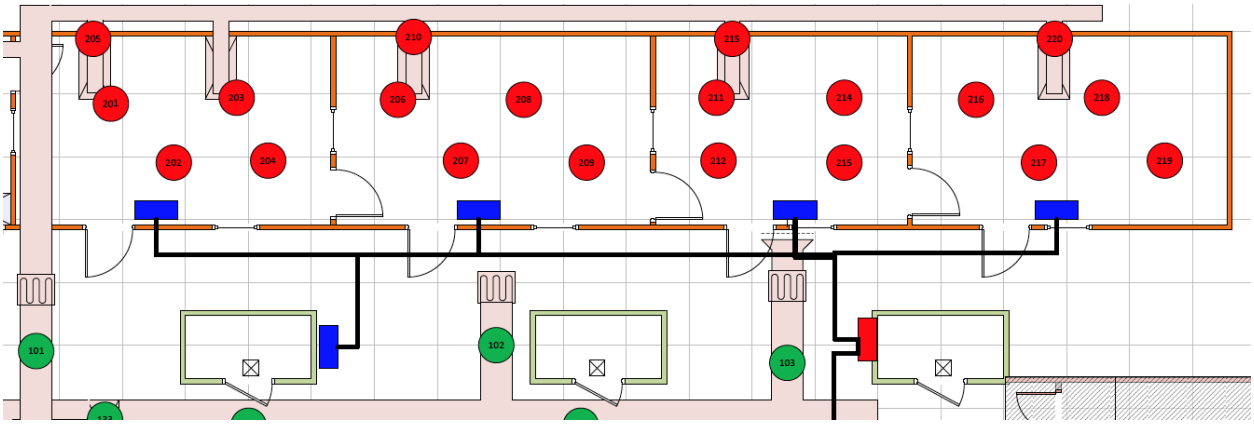


**Figure 14. Schematic of rooms two through five with AeroTrak particle counter numbering**

## 4.2 Data

### *4.2.1 Duct nearest release location*

The 0.3 μm and 0.5 μm channels for AeroTrak 101 are plotted in Figure 15 and Figure 16. The data were normalized by the maximum AeroTrak concentration to provide timing information. The release duration (180 seconds) was taken as the portion of the data greater than 0.8 in normalized concentration.

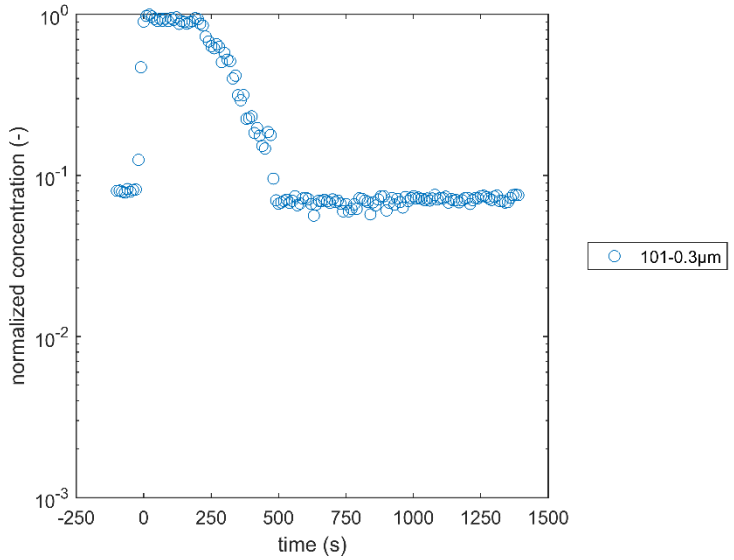


**Figure 15. AeroTrak particle counter data for test S014 in the inlet duct nearest the point of release (Counter 101): 0.3 μm**

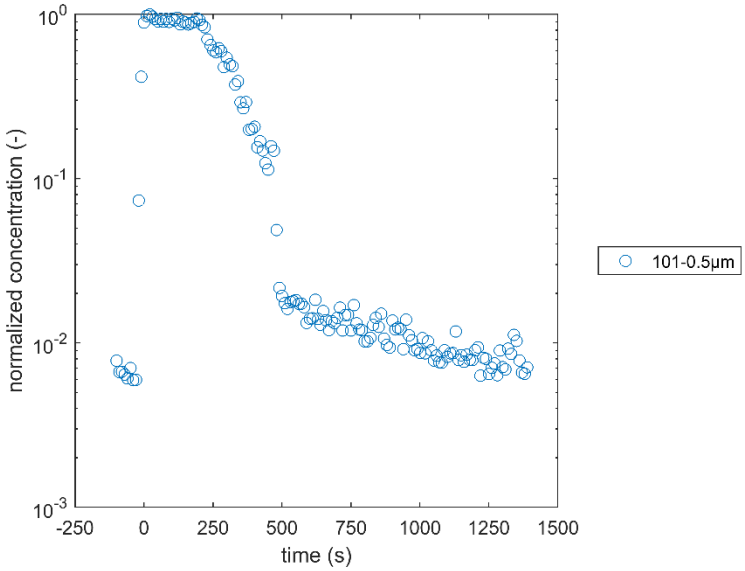


**Figure 16. AeroTrak particle counter data for test S014 in the inlet duct nearest the point of release (Counter 101): 0.5 μm**

### *4.2.2 Compartment 2*

AeroTrak data for compartment 2 are shown below. Counter 205 was located inside the duct, and therefore decayed much faster than the counters in the compartment.

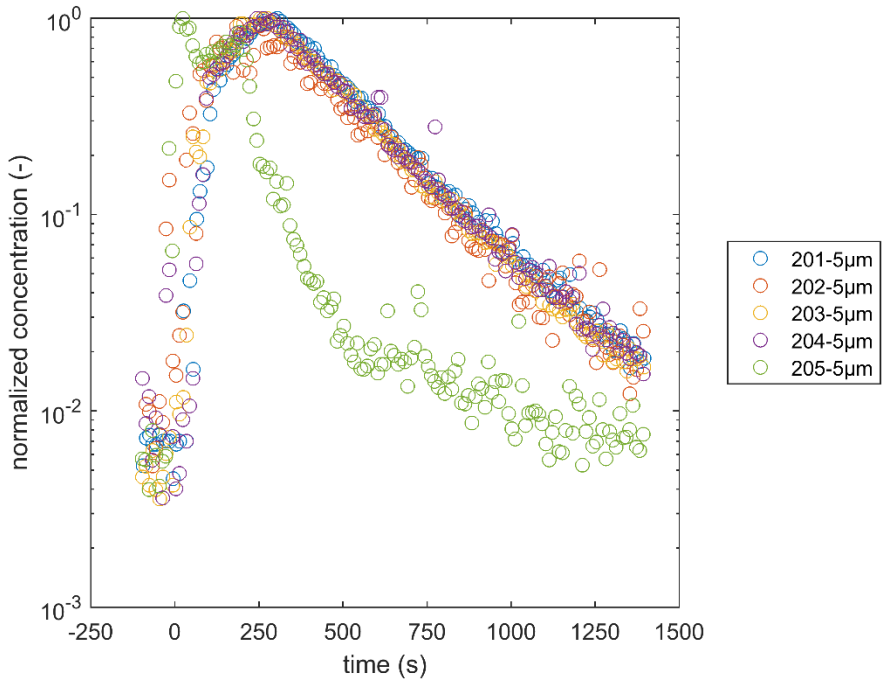


**Figure 17. AeroTrak particle counter data for test S014 in compartment 2: 5.0 μm**

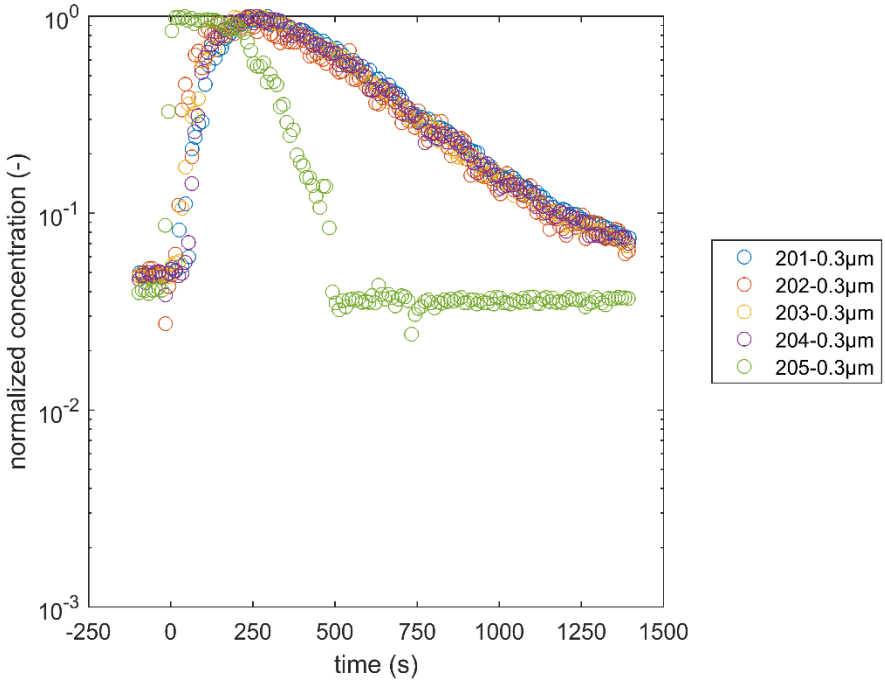


**Figure 18. AeroTrak particle counter data for test S014 in compartment 2: 0.3 μm**

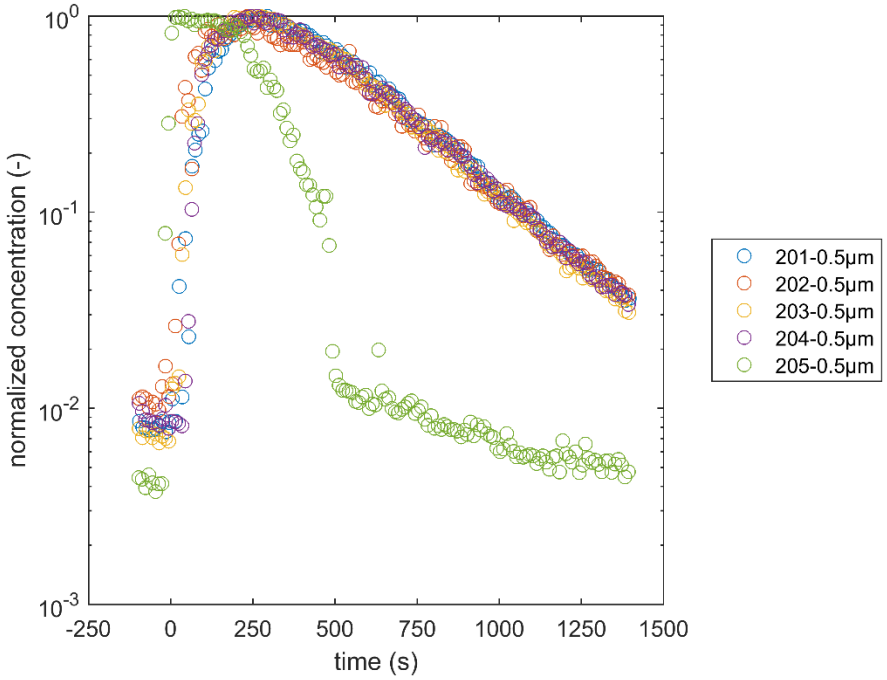


**Figure 19. AeroTrak particle counter data for test S014 in compartment 2: 0.5 µm**

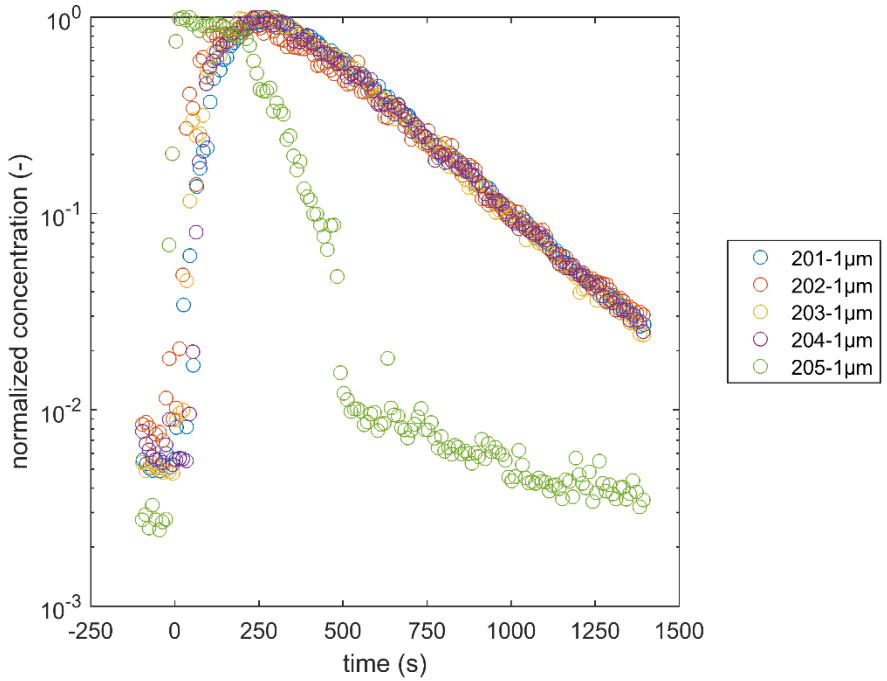


**Figure 20. AeroTrak particle counter data for test S014 in compartment 2: 1.0 µm**

### *4.2.3 Compartment 3*

AeroTrak and APS data were plotted in compartment 3. Good agreement was observed for the shapes of the APS and AeroTrak data for counters 206-209. Counter 210 was located inside the supply duct.

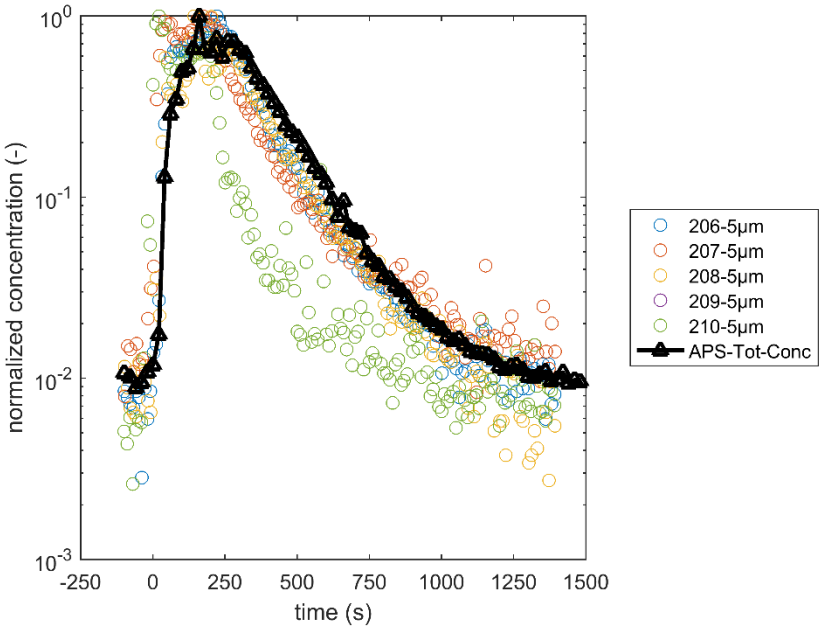


**Figure 21. AeroTrak particle counter data, and Aerodynamic Particle Sizer data for test S014 in compartment 3: 5.0 μm**

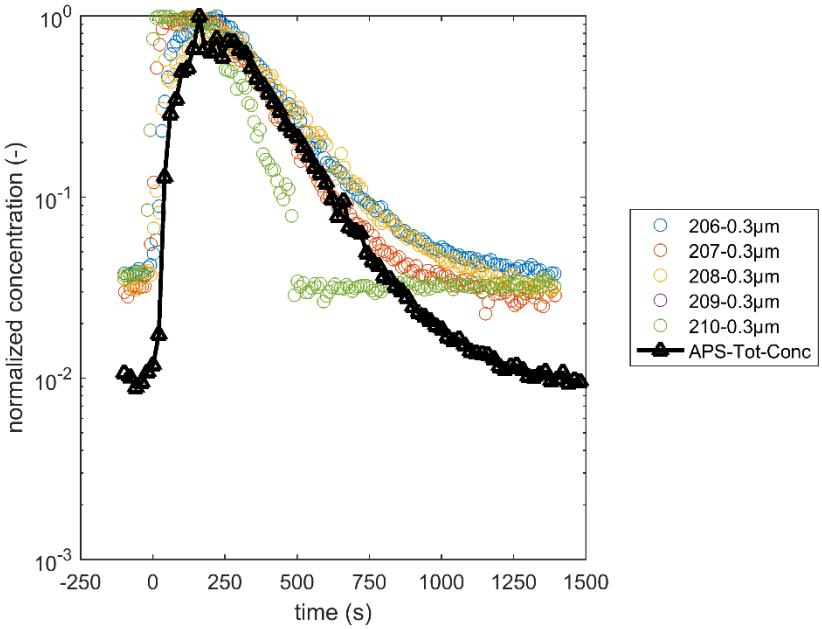


**Figure 22. AeroTrak particle counter data, and Aerodynamic Particle Sizer data for test S014 in compartment 3: 0.3 μm**

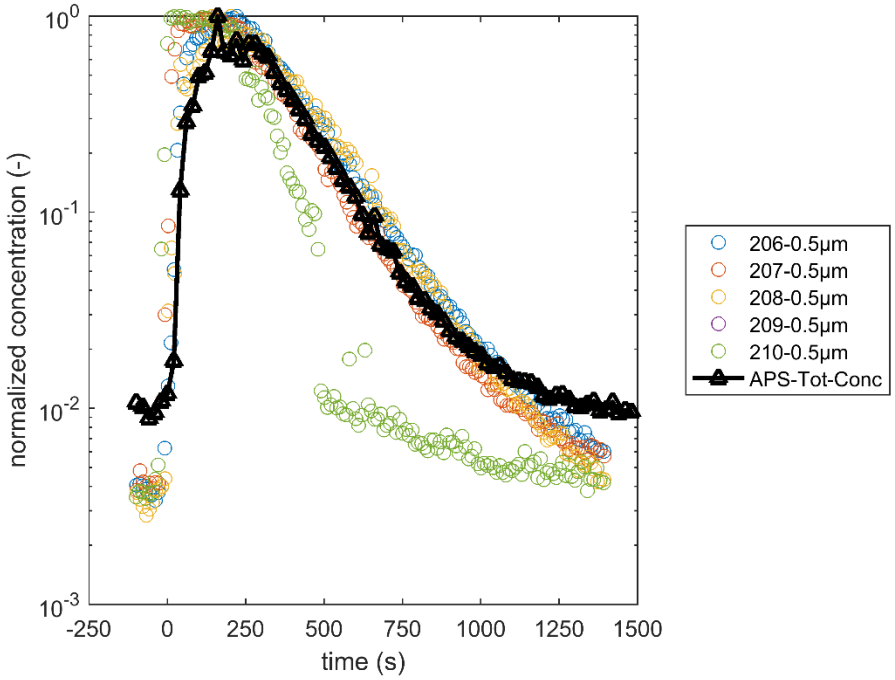


**Figure 23. AeroTrak particle counter data, and Aerodynamic Particle Sizer data for test S014 in compartment 3: 0.5 µm**

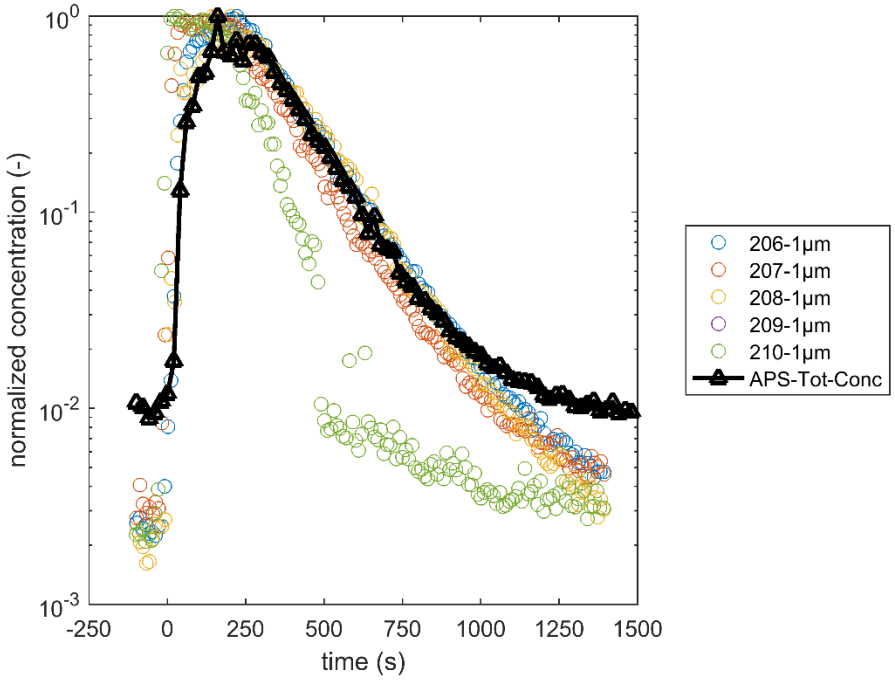


**Figure 24. AeroTrak particle counter data, and Aerodynamic Particle Sizer data for test S014 in compartment 3: 1.0 µm**

### 4.2.4 Compartment 4

Compartment 4 data are shown below but were not used for model validation.

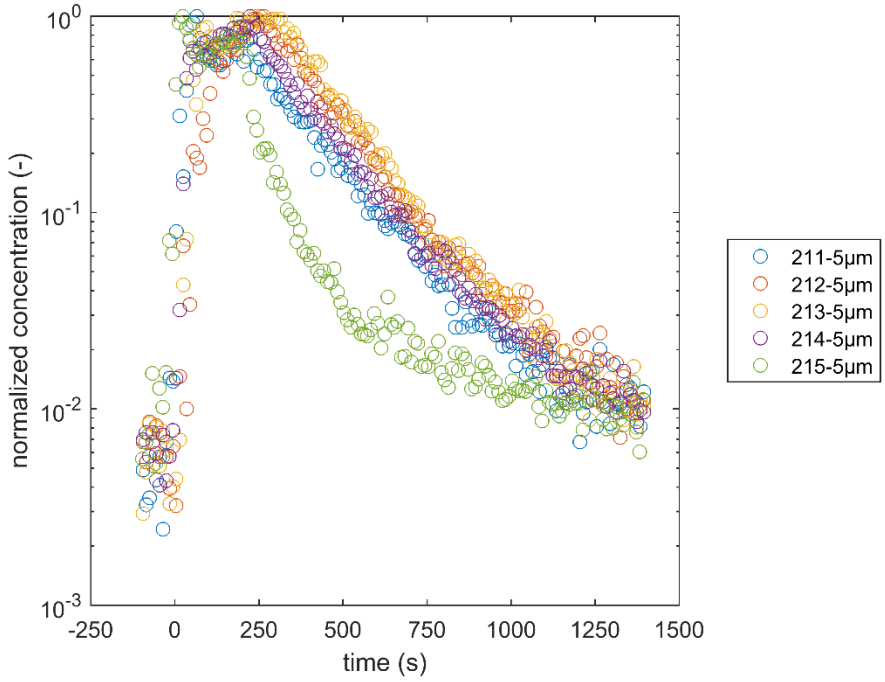


**Figure 25. AeroTrak particle counter data for test S014 in compartment 4: 5.0 μm**

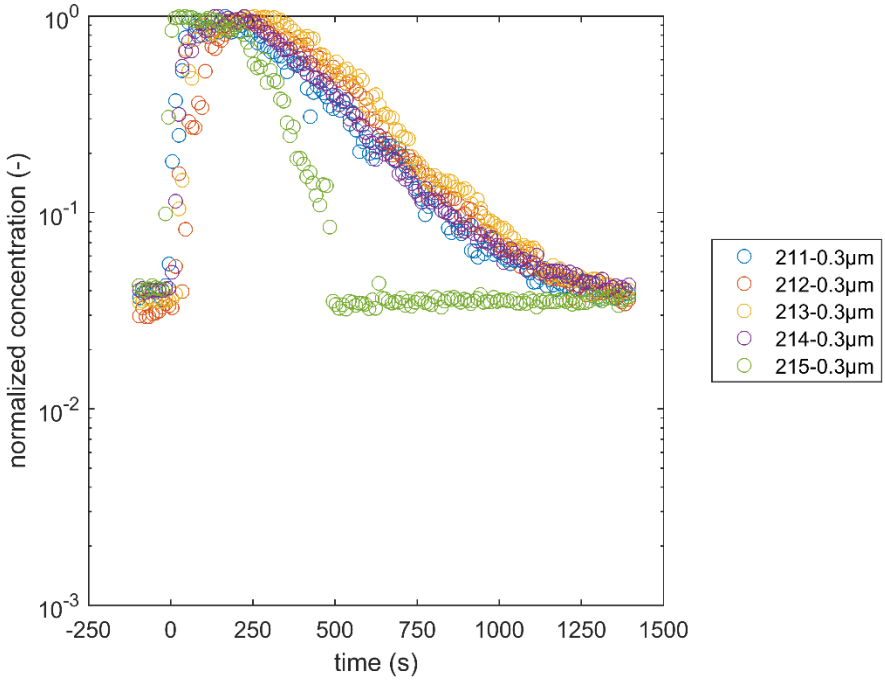


**Figure 26. AeroTrak particle counter data for test S014 in compartment 4: 0.3 μm**

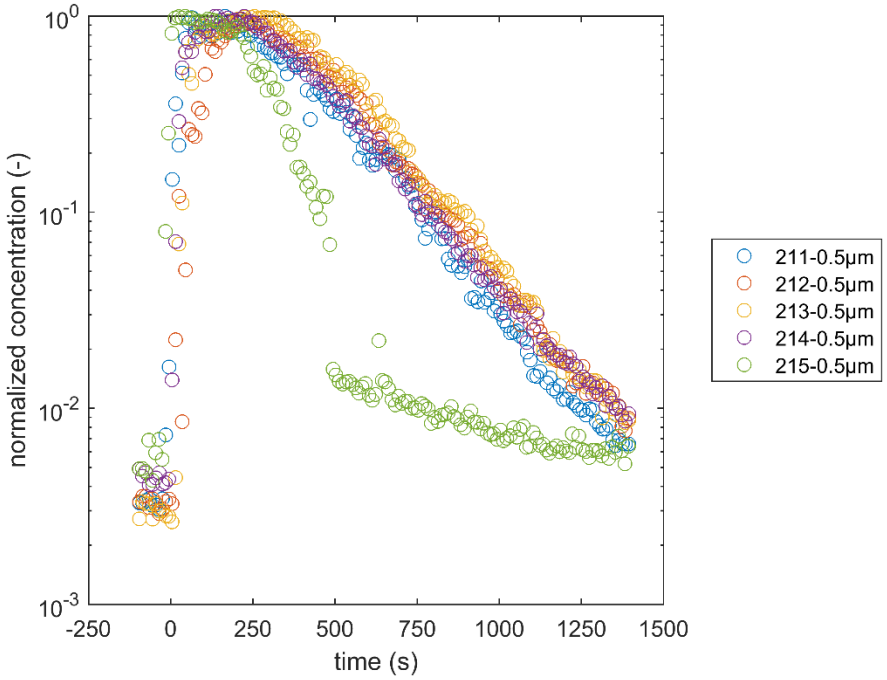


**Figure 27. AeroTrak particle counter data for test S014 in compartment 4: 0.5 µm**

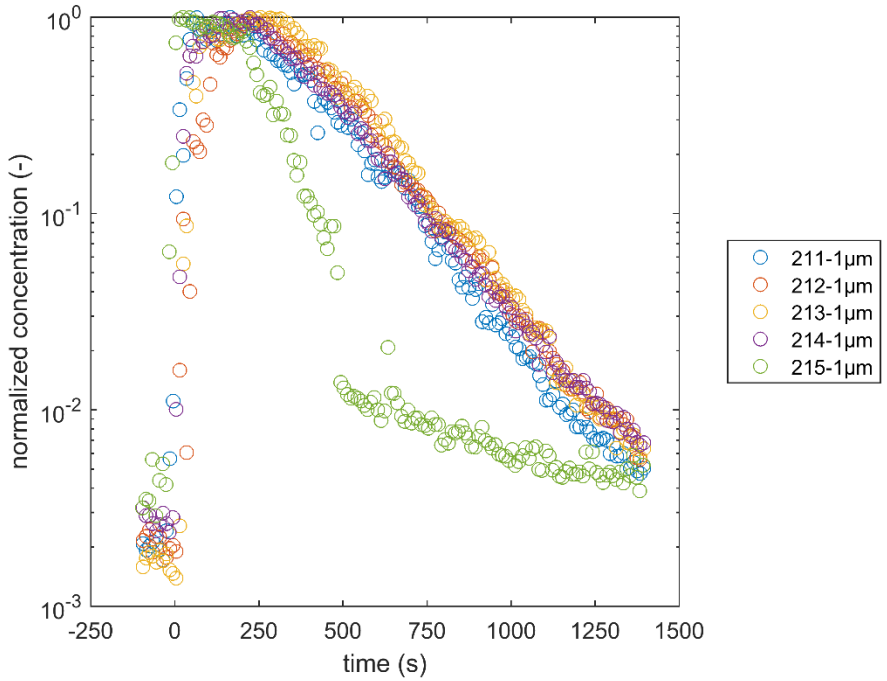


**Figure 28. AeroTrak particle counter data for test S014 in compartment 4: 1.0 µm**

### 4.2.5 Compartment 5

Compartment 5 data are shown below but were not used for model validation.

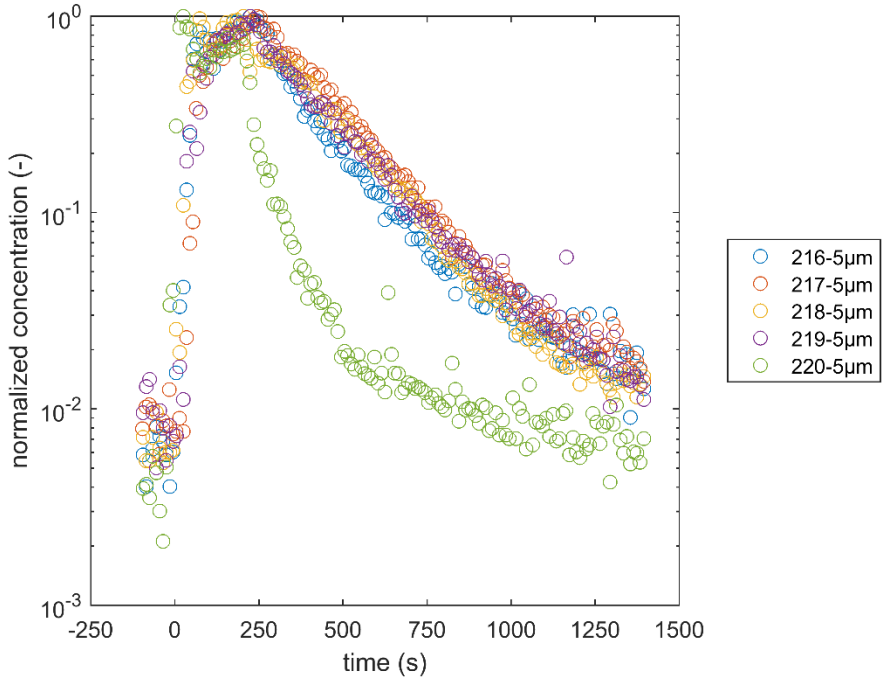


**Figure 29. AeroTrak particle counter data for test S014 in compartment 4: 5.0 μm**

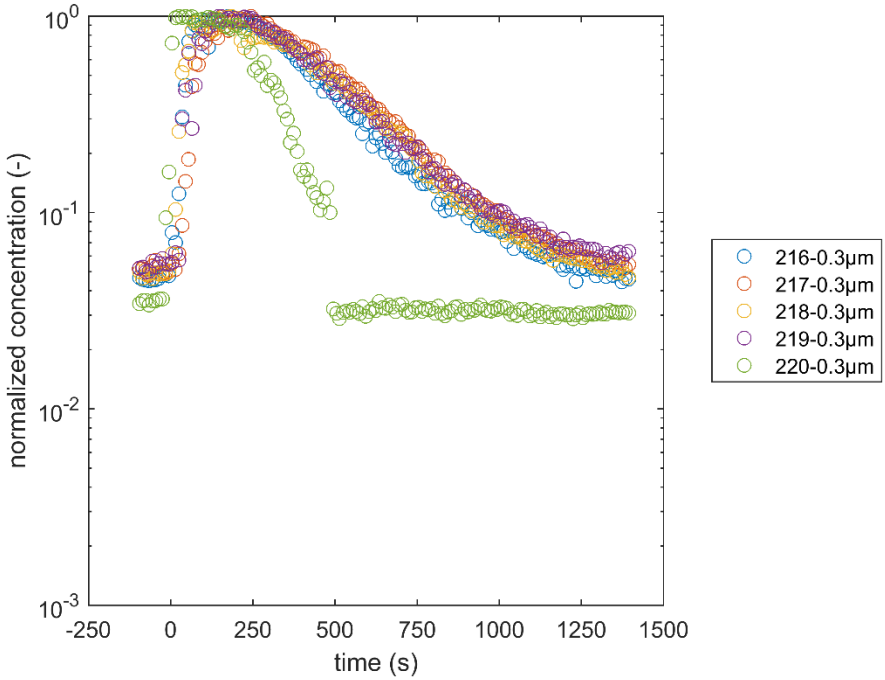


**Figure 30. AeroTrak particle counter data for test S014 in compartment 4: 0.3 μm**

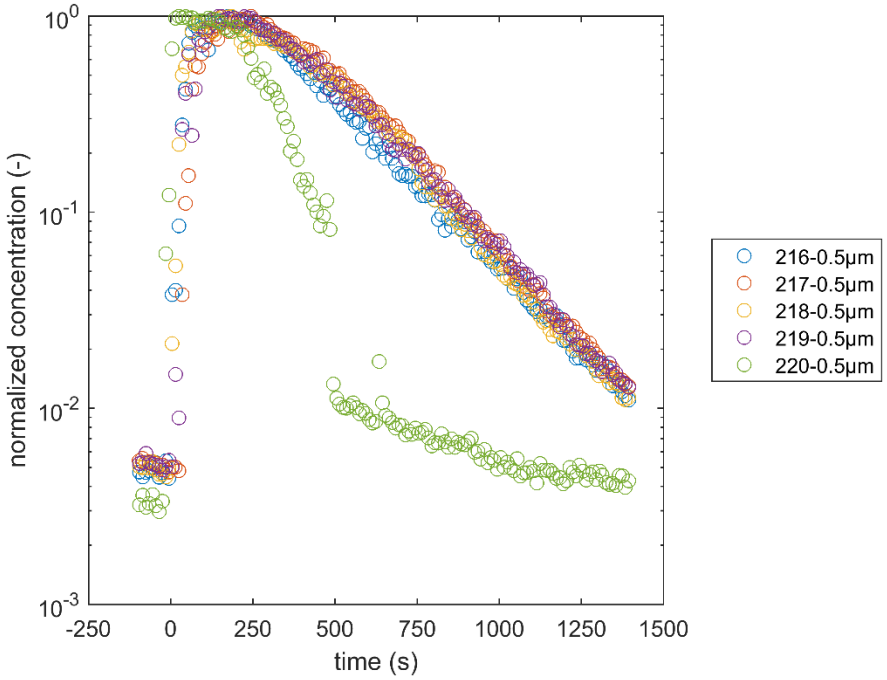


**Figure 31. AeroTrak particle counter data for test S014 in compartment 4: 0.5 µm**

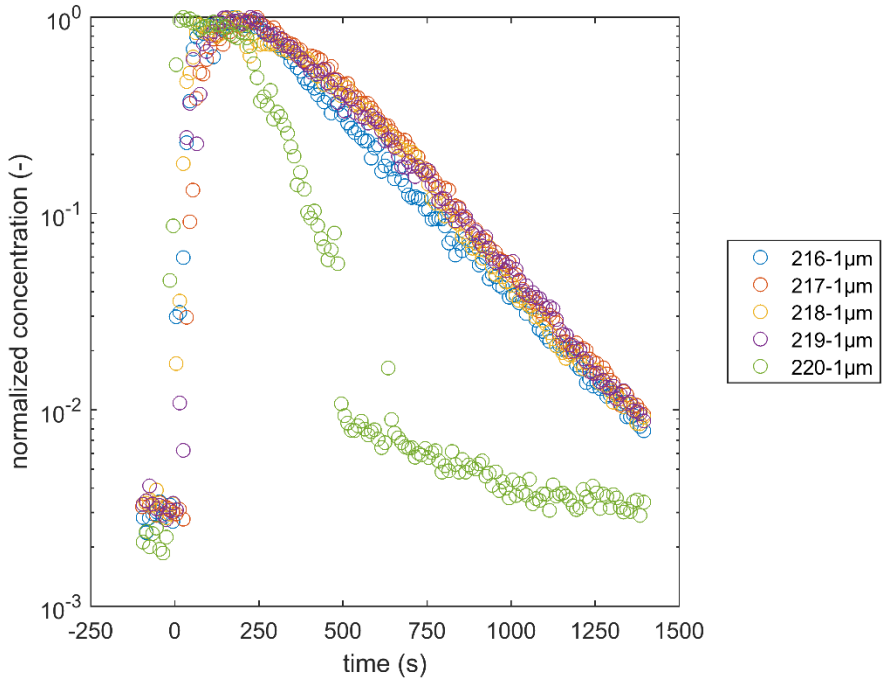


**Figure 32. AeroTrak particle counter data for test S014 in compartment 4: 1.0 µm**

## 4.3 Validation Cases

### *4.3.1 Approach*

The total powder mass released ($m_{total}$) was normalized by the particle mass ($m_p$) to give the total number of particles in the powder mass. The total mass released was not always recorded but was consistently 6-8 grams of $TiO_2$ in other tests. Approximately 10% of the total mass was fluidizer and was not assumed to affect the overall particle size distribution. The total number of particles in the powder mass was then divided by the total air flow volume which was calculated as the product of total air flow rate ($Q_0$) and release duration ($t_{release}$) of 180 seconds.

$$C_i = \frac{\left(\frac{m_{total}}{m_p}\right)}{Q_o \cdot t_{release}} = \frac{\left(\frac{m_{total}}{\frac{\pi}{6}\rho_p d_e^{\,3}}\right)}{Q_o \cdot t_{release}} \qquad \text{* MERGEFORMAT (27)}$$

The inlet-duct concentration calculation is sensitive to volume equivalent particle diameter ($d_e$). A factor of two difference in particle diameter results in a factor of 8 change in the inlet-duct concentration.

The mass mean aerodynamic diameter, $d_a$, was measured with the TSI Aerodynamic Particle Sizer in compartment 3. The mass mean volume equivalent diameter, $d_e$, was then calculated with the following conversion factor:

$$d_e = \frac{d_a}{\sqrt{\frac{\rho_p}{\rho_0}}}. \qquad \text{* MERGEFORMAT (28)}$$

In * MERGEFORMAT (28), $\rho_p$ and $\rho_0$ are the true particle density (4.23 g/cc) and standard particle density (1 g/cc). For this $TiO_2$ powder, the volume equivalent diameter was approximately half the size of the aerodynamic diameter. We assumed that the only losses in the ductwork were gravitational losses and that all aerosol released was entrained in the duct flow. Inertial transport losses in duct bends could be incorporated in future model releases.

### 4.3.2 Inlet-Duct Concentrations Calculated with Compartment 3 PSD

Aerodynamic Particle Sizer data was used to characterize the aerosol in Compartment 3. One measurement from the test duration is shown in Figure 33.

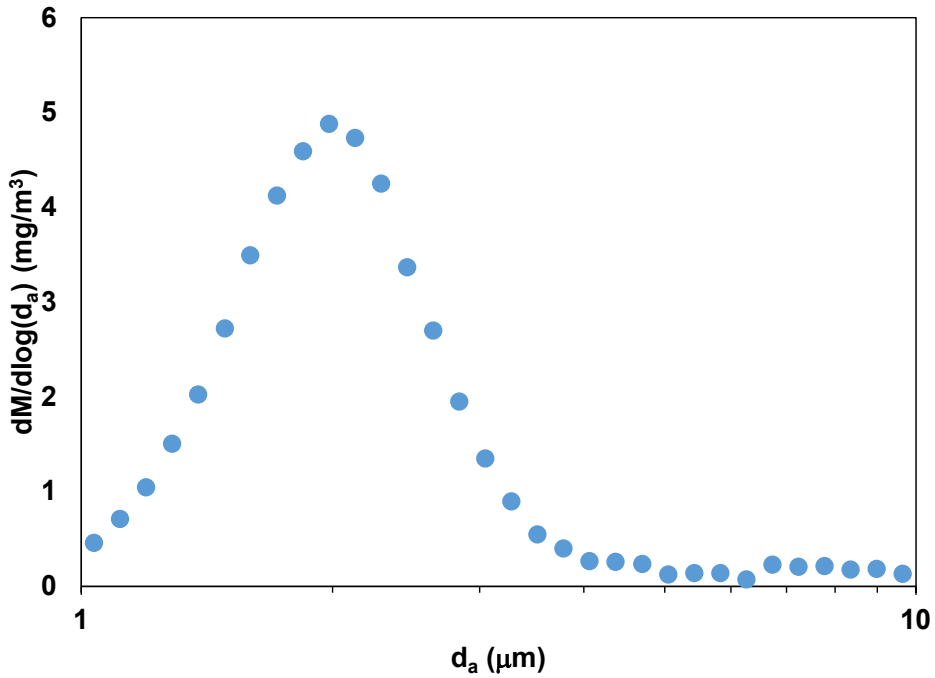


**Figure 33. Aerosol mass concentration as a function of aerodynamic diameter for $TiO_2$ in compartment 3**

The mass mean aerodynamic diameter, $d_a$, of 2.25 μm was converted into mass mean volume equivalent diameter, $d_e$, of 1.09 μm. Model results for Compartment 3 number concentration as a function of time are shown below. The total number concentration is over-estimated when total powder mass is assumed to be distributed amongst 1.09 μm particles.

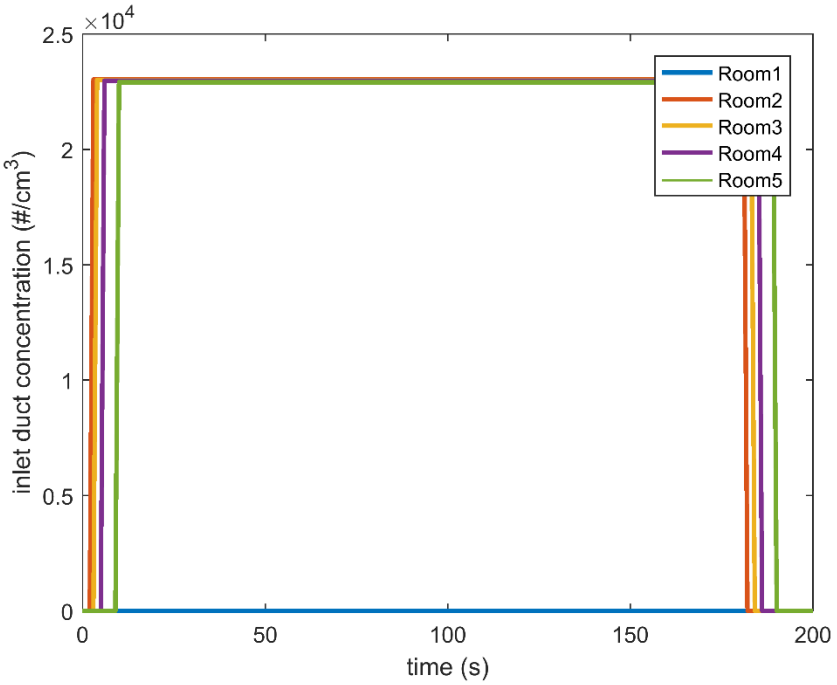


**Figure 34. Calculated inlet duct concentration profiles for S014 incorporating effects of time delays and transport losses in the ductwork. Model data assume $m_{total}$ = 6.3 g, $d_e$ = 1.09 µm. Intercompartment transport terms were set to zero since no DP data were available.**

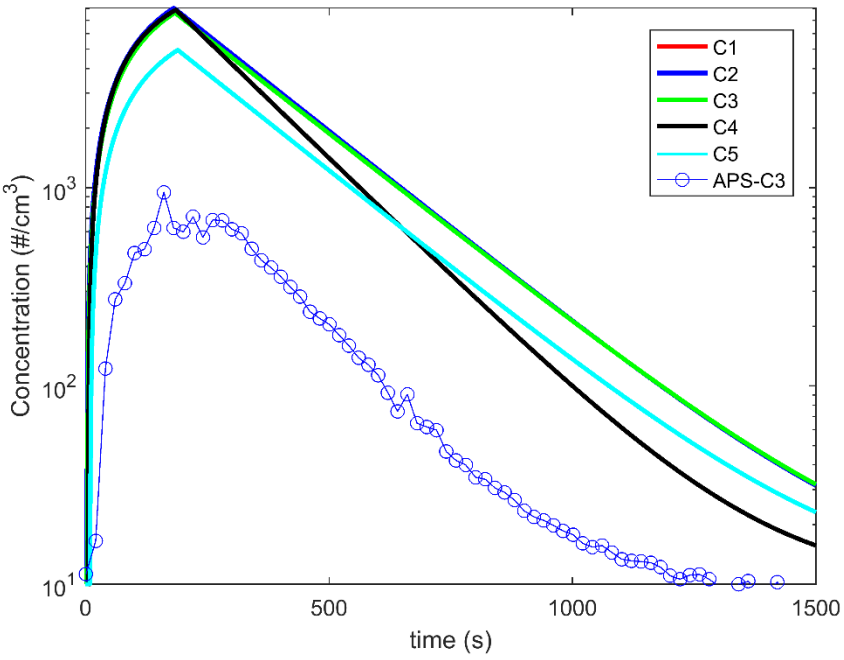


**Figure 35. Aerosol concentration vs. time. Experimental data shown for compartment 3 where an Aerodynamic Particle Sizer was used to measure the total aerosol concentration. Model data assume $m_{total}$ = 6.3 g, $d_e$ = 1.09 µm. Intercompartment transport terms were set to zero since no DP data were available.**

### 4.3.3 *Inlet-duct Concentration Calculations with Upstream Approximation for $d_e$*

Losses upstream of the compartment (in the ductwork) likely skewed the distribution before it was measured within the compartment. The mass mean volume equivalent diameter before duct transport should be used to calculate the inlet-duct concentrations. Test data was available from a stand-alone aerosol generation test where the measured aerosol was not transported through ductwork. Data are shown in Figure 36. It is apparent that the mass mean volume equivalent diameter is above 1.09 μm. Particle counts in the stand-alone test were low at larger particle sizes (> 5 μm). We use this data to justify allowing the model particle diameter to vary to represent experimental data.

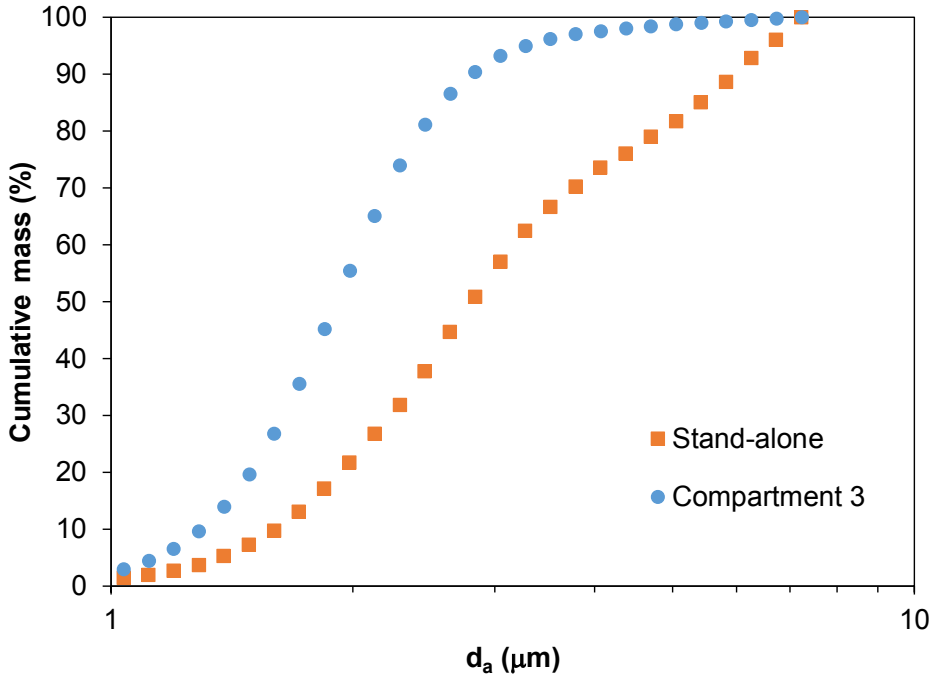


**Figure 36. Cumulative mass percent for APS data taken in Compartment 3 (after aerosol transport through ductwork) and in a stand-alone experiment (without aerosol transport through ductwork)**

If the volume equivalent diameter is allowed to vary in the model, a diameter of 2.3 μm gives good agreement with experimental data. We held $m_{total}$ constant at 6.3 grams (90% of 7 grams). Model data are shown below for $d_e$ = 2.3 μm. Much better agreement was observed.

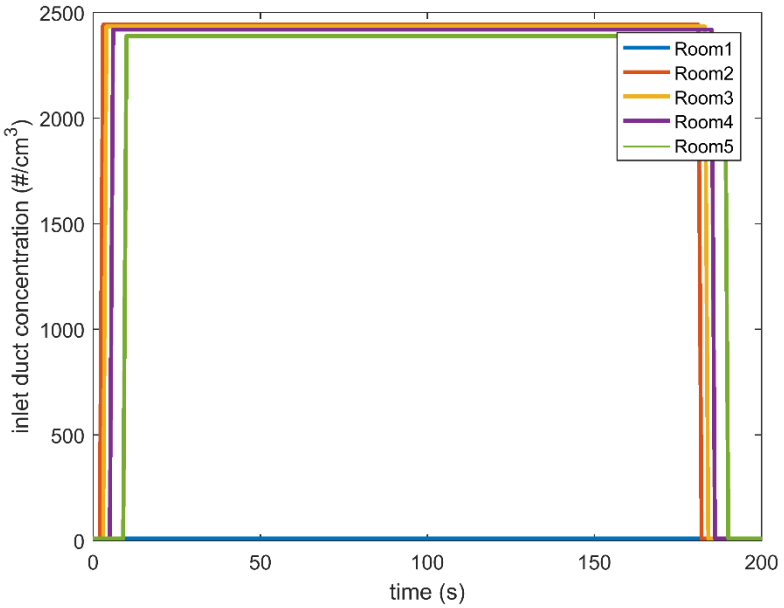


**Figure 37. Calculated inlet duct concentration profiles for S014 incorporating effects of time delays and transport losses in the ductwork. Model data assume $m_{total}$ = 6.3 g, $d_e$ = 2.3 μm. Intercompartment transport terms were set to zero since no DP data were available.**

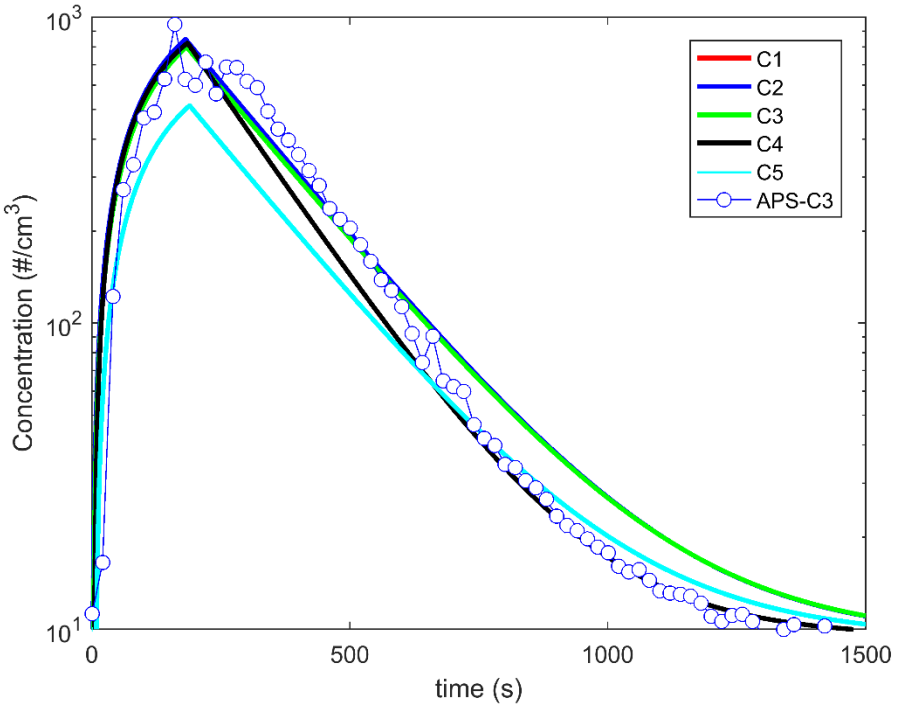


**Figure 38. Aerosol concentration vs. time. Experimental data shown for compartment 3 where an Aerodynamic Particle Sizer was used to measure the total aerosol concentration. Model data assume $m_{total}$ = 6.3 g, $d_e$ = 2.3 μm. Intercompartment transport terms were set to zero since no DP data were available.**

### 4.3.4 *Inlet-duct Concentration Calculations with Approximations for $d_e$ and Intercompartment flows*

No intercompartmental pressure drop measurements were made for the validation test case. Here we assumed reasonable values to determine the effects of including intercompartmental transport on model solutions: $DP_{12}$ = 0 Pa, $DP_{23}$ = 3 Pa, $DP_{34}$ = 3 Pa, $DP_{45}$ = 3 Pa. These pressure drops gave intercompartmental transport flow rates on the same order of the inlet-duct flow rates (~0.1 $m^3/s$). Model and experimental data are shown in Figure 39. The rate of decay of compartment 3 concentration ($C_3$) increased, more closely matching experimental data (APS-$C_3$). The rate of decay of compartment 5 concentration ($C_5$) decreased with respect to model results not including intercompartmental transport. Model results for compartment 3 were within 25-30% of the experimental data. Parameters used in this validated model simulation are given in Table 1.

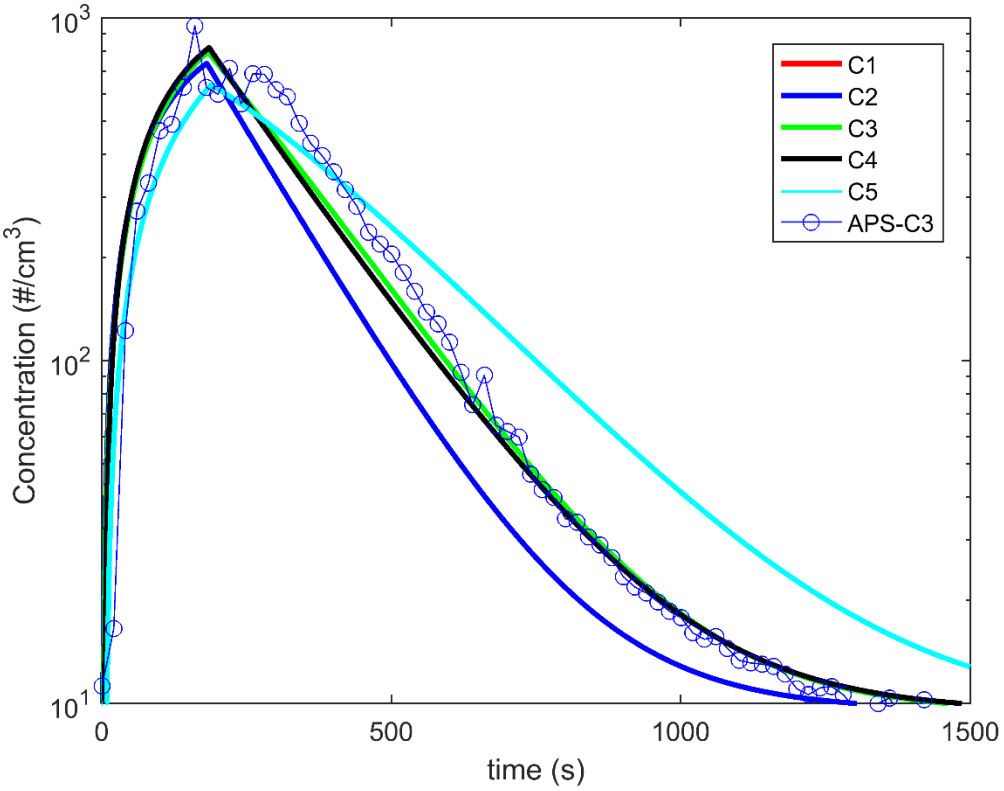


**Figure 39. Aerosol concentration vs. time. Experimental data shown for compartment 3 where an Aerodynamic Particle Sizer was used to measure the total aerosol concentration. Model data assume $m_{total}$ = 6.3 g, $d_e$ = 2.3 µm. Intercompartment transport terms were calculated using the following hypothetical pressure differentials: $DP_{12}$ = 0 Pa, $DP_{23}$ = 3 Pa, $DP_{34}$ = 3 Pa, $DP_{45}$ = 3 Pa.**

**Table 1. Compartment and intercompartment parameters utilized for final model validation**

| Compartment | Units | 1 | 2 | 3 | 4 | 5 |
|---|---|---|---|---|---|---|
| V | ($m^3$) | 10.5622 | 54.6232 | 54.6232 | 43.6079 | 54.6232 |
| A | ($m^2$) | 4.3316 | 22.4012 | 22.4012 | 17.8838 | 22.4012 |
| $\rho_p$ | ($kg/m^3$) | 4320 | 4320 | 4320 | 4320 | 4320 |
| $d_e$ | (m) | 2.30E-06 | 2.30E-06 | 2.30E-06 | 2.30E-06 | 2.30E-06 |
| $m_{total}$ | (kg) | 0.0063 | 0.0063 | 0.0063 | 0.0063 | 0.0063 |
| $Q_i$ | ($m^3/s$) | 0 | 0.1557 | 0.1463 | 0.1312 | 0.0958 |
| $Q_o$ | ($m^3/s$) | 0 | 0.2416 | 0.2388 | 0.2364 | 0.2431 |
| $Q_m$ | ($m^3/s$) | 0 | 0.1887 | 0.0925 | 0.1052 | 0.0445 |
| $Q_{recirc}$ | ($m^3/s$) | 0 | 0 | 0 | 0 | 0 |
| $\eta$ | (-) | 1 | 1 | 1 | 1 | 1 |
| $C_{initial}$ | ($\#/m^3$) | 1.00E+07 | 1.00E+07 | 1.00E+07 | 1.00E+07 | 1.00E+07 |
| $C_{bg}$ | ($\#/m^3$) | 1.00E+07 | 1.00E+07 | 1.00E+07 | 1.00E+07 | 1.00E+07 |

| Intercompartment | Units | 12 | 23 | 34 | 45 |
|---|---|---|---|---|---|
| DP | (Pa) | 0 | 3 | 3 | 3 |
| Q | ($m^3/s$) | 0 | 0.1028 | 0.1028 | 0.1028 |

# 5 SUMMARY

A well-mixed, multi-zone, aerosol transport model was developed, verified, and validated for a five-compartment cleanroom facility. Each compartment included ventilation, intercompartment transport, and gravitational settling. The set of governing coupled ordinary differential equations was derived from conservation of mass. The coupled set of ODEs was then solved in MATLAB. Model verification was performed with test cases of (1) constant inlet-duct concentration, and (2) exponentially decaying inlet-duct concentration. Normalized errors of less than $10^{-9}$ were calculated by comparing model and analytical solutions. The model was validated against a single experiment. Model results were within 25-30% of experimental data when reasonable approximations were made for the initial particle mean volume equivalent diameter and intercompartment pressure differentials.

# REFERENCES

Brockmann (2001). *Aerosol Transport in Sampling Lines and Inlets*, in Aerosol Measurement: Principles, Techniques, and Applications, 3rd Edition.

Hubbard and Knowlton (2015). Indoor-Outdoor Aerosol Transport Model Used for Hazard Assessment. Sandia National Laboratories, Albuquerque, New Mexico. Report SAND2015-9599.

Trost and Hubbard (2012). Aerosol Transport in Mass Transit Facilities. Sandia National Laboratories, Albuquerque, New Mexico. Report SAND2012-7630.

Walker, Wilson, and Sherman (1998). A comparison of the power law formulations for air infiltration calculations. Energy and Buildings (27) 293-299.

# DISTRIBUTION

| Quantity | Mailstop | Person | Organization |
|---|---|---|---|
| 1 | MS0899 | Technical Library | 10756 |
| 1 | MS0968 | Josh Hubbard | 05754 |
| 1 | MS0968 | Michael Omana | 05754 |
| 1 | MS1148 | Josh Santarpia | 06633 |
| 1 | MS1148 | Danielle Rivera | 06633 |
| 1 | MS1148 | Gabe Lucero | 06633 |
| 1 | MS1455 | Chris Brotherton | 02555 |


Sandia National Laboratories